ADDIS ABABA UNIVERSITY

COLLEGE OF HEALTH SCIENCES

SCHOOL OF PHARMACY

DEPARTMENT OF PHARMACEUTICS AND SOCIAL PHARMACY

IRON OXIDE NANOPARTICLES SYNTHESISED USING BANANA PEELS *(MUSA SPP.)* EXTRACT FOR DELIVERY OF CIPROFLOXACIN AGAINST RESISTANT *ESCHERICHIA COLI*

By:

AYCHEW MEKURIAW TEGEGNE

October, 2023

Addis Ababa, Ethiopia.

Iron oxide nanoparticles synthesized using banana peels *(Musa spp.)* extract for delivery of ciprofloxacin against resistant *Escherichia coli*

By:

Aychew Mekuriaw Tegegne

A Thesis Submitted to the Department of Pharmaceutics and Social Pharmacy, School of Pharmacy, College of Health Science, Addis Ababa University for the Partial Fulfillment of the Requirements of the Degree of Master of Science in Pharmaceutics.

Supervised by

Gebremariam Birhanu (Ph.D.) and Muluken Nigatu (Asst. Prof.), Department of Pharmaceutics and Social Pharmacy, School of Pharmacy, Addis Ababa University

October, 2023

Addis Ababa, Ethiopia.

Declaration

I, the person signing, hereby certify that the thesis titled "Iron oxide nanoparticles synthesized using banana peels (*Musa spp*.) extract for ciprofloxacin delivery against resistant *E. coli*" is the result of my own investigation and was not done in substance for the conferral of any degree at any other institution. Every source of resources utilized in this thesis has been properly credited.

	Signature	Date
Aychew Mekuriaw Tegegne	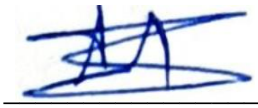	03/10/2023

Addis Ababa University

School of Graduate Studies

This is to certify that the thesis prepared by Aychew Mekuriaw Tegegne, entitled: 'Iron oxide nanoparticles synthesized using banana peels (*Musa spp*.) extract for delivery of ciprofloxacin against resistant *Escherichia coli*' and submitted for the partial fulfillment of the requirements for the degree of Master of Science in Pharmaceutics complies with the regulations of the University and meets the accepted standards with respect to originality and quality.

Approved and signed by the examining committee:

Name	Signature	Date
1. Dr. Gebremariam Birhanu (Advisor)		07-Oct-23
2. Mr. Muluken Nigatu (Advisor)		10-10-23
3. Dr. Muluneh Fromsa (External Examiner)	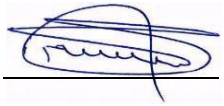	09-10-2023
4. Dr. Nisha M. Joseph (Internal Examiner)		

Abstract

Resistance to antimicrobials is one of our most significant worldwide challenges. In Africa, around 31% of the infections of urinary tract (UTIs) initiated by *Escherichia coli* (*E. coli*) have been observed to develop ciprofloxacin (CIP) resistance. As a result, significant efforts have been made to investigate novel and improved antibiotics. Nanoparticles (NPs) have been shown to have significant efficacy in medication delivery against multidrug-resistant (MDR) strains of the bacteria. Green synthesized metal oxide NPs using plant extract is eco-friendly, biocompatible, less toxic, cost-effective and rapid method to control such emergent. This study aimed at synthesizing iron oxide nanoparticles (IONPs) using banana peels (*Musa Spp*.) extract for delivery of CIP against resistant *E. coli*. The preparation of IONPs was done by green synthesis method. The extract of banana peels was employed as an agent of reduction and stabilization for the precursor ions of iron used in the manufacture of IONPs. Fourier-transform infrared (FTIR) spectroscopy, Dynamic light scattering (DLS), X-ray diffraction (XRD), ultraviolet-visible spectrophotometer (UV-vis), scanning electron microscopy (SEM), and differential thermal gravimetry (DTG) were used to characterize the manufactured and medication-loaded IONPs. DLS, UV-vis, and FTIR were once utilized to assess load capacity and encapsulating capability of IONPs. CIP-IONPs were evaluated for its efficient release of the loaded drug in three different simulation media using UV-vis spectrophotometer and for its *in vitro* antimicrobial susceptibility. The formation of hematite (α-Fe_2O_3) was confirmed with its FTIR characteristic peak for it at 461cm^{-1}, 542cm^{-1} and 1131cm^{-1}. The size of synthesized IONPs were found to be 10.4nm $\pm$ 1.98, 48nm $\pm$ 0.9 and 67.3nm $\pm$ 0.9 under XRD, SEM and DLS measurements respectively. CIP-IONPs had almost the maximum drug loading capacity (33.3% $\pm$ 0.67) with fast and slow drug release pattern at gastric and intestinal or blood pH respectively. The antimicrobial susceptibility study also showed a significant resistance reversal effect for ciprofloxacin resistant *E. coli*. Green synthesized IONPs were produced efficiently using a banana peels extract. It had a recommended characteristics and application. And it will be a good alternative in alleviating the emergent CIP resistant *E. coli*.

Key words: Antimicrobial resistance, Green synthesis, Iron oxide nanoparticles, Ciprofloxacin, Banana peels extract, *E. coli*.

I. Acknowledgments

I want to convey my deepest appreciation to my advisers, Dr. Gebremariam Birhanu and Mr. Muluken Nigatu, for their insightful remarks and consistent follow-up from the proposal preparation through the finished thesis work. My acknowledgment also goes to the Department of Pharmaceutics and Social Pharmacy, Addis Ababa University and Debre Berhan University for providing this thesis work that helped me to get the experience of literature compilation and sponsoring of my Msc program respectively.

I would like to acknowledge Dr. Yitayal Admasu, Dr. Eyobel Mulugeta and my seniors Mr. Mesay Wondaya and Ms. Lielt Belete for their impressive and encouraging consultation on my dissertation work.

I'd want to express my heartfelt appreciation.for Humanwell Pharmaceutical Industry Ethiopia, and Chemical Engineering Department and Asrat Woldeyese Health Science College of Debre Berhan University for their incredible support by providing ciprofloxacin HCL active ingredient (Humanwell Pharmaceutical Industry Ethiopia), and allowing me to accomplish different test in their facility (all of the institutions).

I'd like to thank Dr. Tesfaye Gebrial for his assistance in providing a dialysis membrane for an *in vitro* drug release investigation. And I want to thank my teachers, friends, and family for their encouragement and support.

II. Table of Contents----------pages

III. Acronyms/Abbreviations

AMR: Antimicrobial Resistance

CFU: Colony Forming Unit

CIP: Ciprofloxacin

CIP-IONPs: Ciprofloxacin loaded Iron Oxide Nanoparticles

CLSI: Clinical and Laboratory Standard Institute

CSA: Central Statistical Agency of Ethiopia

DLS: Dynamic Light Scattering

DTG: Differential Thermal Gravimetry

E. coli: Escherichia Coli

ETC: Electron Transport Chain

FTIR: Fourier-Transform Infrared

IONPs: Iron Oxide Nanoparticles

KBr: Potassium Bromide

MDR: Multi-Drug Resistance

MNPs: Magnetite Nanoparticles

NPs: Nanoparticles

PBS: Phosphate-Buffered Saline

PCL: Polycaprolactone

PDI: Polydispersity Index

SEM: Scanning Electron Microscopy

TEM: Transmission Electron Microscopy

TGA: Thermogravimetric Analysis

UTIs: Urinary Tract Infections

UV-Vis: Ultra Violet -visible spectrophotometer

XRD: X-Ray Diffraction

ZOI: Zone of Inhibition

IV. List of Tables

V. List of Figures

1. Introduction

1.1. Background

1.1.1. Antimicrobial resistance

Antimicrobials have long been a cornerstone of human health, having been extensively utilized to treat infections of respiratory tract, bacterial infestation of the urinary tract, gastrointestinal infections, and nervous system infections (Vassallo et al., 2020). Nevertheless, the rise of multidrug-resistant pathogens (MDR) different strains of the bacteria have severely compromised their effectiveness (Singh et al., 2014). AMR happens due to microorganisms including viruses, bacteria, parasites, and fungi get the ability to adjust themselves to raise and grow in the existence of medicines that once impacted them (Ibrahim et al., 2023).

Microbes that cause AMR Infection sets the stage for catastrophic diseases and prolonged hospitalizations, which raise healthcare costs, expose patients to second-line medications, and result in treatment failures (Shrestha et al., 2018). As an illustration, in Europe, AMR is expected to cost in excess of nine billion euros each year (Founou et al., 2017). Furthermore, in accordance with the CDC stands for the Centers for Disease Control and Prevention, AMR raises direct healthcare expenses by a total of twenty billion dollars in the USA alone (US Department of Health and Human Services, 2019). As a result, It's also one of among the most important worldwide challenges, and significant attempts have been made to discover innovative and sophisticated antibiotics (Vassallo et al., 2020)..

1.1.1.1. Urinary tract infections (UTIs)

UTIs are among the most prevalent antibiotic-resistant infections globally, mostly caused by Gram-negative bacteria such as *E. coli*, and *Proteus species*. However, Gram-positive bacteria, *Staphylococcus saprophyticus*, and *Enterococcus species*, are part of the typical predictable spectrum of bacteria that cause UTIs (Sultana and Toaha, 2021).

It is the common health problem difficult to treat with antibiotics due to antibiotics resistance both in the community and in the hospital settings. According to Ahmed *et al*., antibiotic resistance was detected in 92% of the urine specimens that tested positive for UTI (Ahmed et al., 2019).

It is one the widespread and the most frequent illnesses, especially among women (Chakupurakal *et al*., 2010). Approximately 50-60% of all women have UTI for a minimum of at some point during their lives (Medina and Castillo-Pino, 2019).

A systematic review reported that *E. coli* was the most predominant uropathogen caused approximately 68-77% of recurrent UTIs (Belete and Saravanan, 2020), and the other study also revealed that it was the most predominant uropathogen of UTIs about 75%–95% (Vol et al., 2022). Most studies agreed on the fact that more than half of the UTIs are initiated by *E. coli* (Ahmed et al., 2019). Rossignol et al. discovered that *E. coli* was the most prevalent pathogen in 393 urine samples with bacteriuria (82.8%), succeeding by *Proteus mirabilis* (4.3%) (Rossignol et al., 2017).

1.1.1.2. Ciprofloxacin

Ciprofloxacin [1-cyclopropyl-6-fluoro-1,4-dihydro-4-oxo-7-piperazinylquinolone-3-carboxylic acid] (CIP) (Figure1) is a frequently prescribed broad spectrum fluoroquinolone used to combat a wide range of bacterial illnesses in the digestive system, urinary tract, lung, joints, bones, skin, and teeth (Herizchi et al., 2016). It is a widely used antibiotic for UTI and is known to work by preventing the type 2 bacterial DNA topoisomerases, DNA gyrase, and topoisomerase IV, due to the production of oxidative radicals that cause the death of bacterial cells and are now the most vital areas in contribution of quinolone resistance (Masadeh et al., 2015).

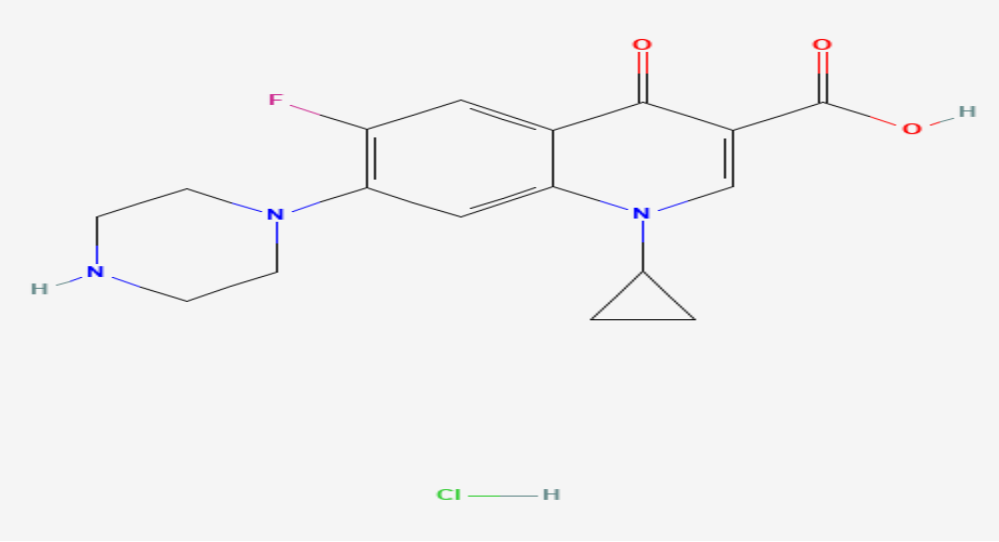

Figure 1: Chemical structure of CIP HCl
(Source: https://pubchem.ncbi.nlm.nih.gov/compound/Ciprofloxacin-Hydrochloride)

There has been a pronounced deal of investigation on the manners behind CIP resistance in *E. coli* over the past 30 years. *E. coli* resistance to CIP is caused through changes in the topoisomerase IV genes and DNA gyrase (Azargun et al., 2019). Furthermore, drug deposits may be reduced via efflux pumps whereas enzymes and peptides, respectively, may cause drug change or inhibit drug targets (Hooper and Jacoby, 2015).

Among the various bacteria that acquire resistance to CIP, the emergence of *E. coli* resistant to CIP is one of the commonest incidents worldwide, with the highest CIP resistance in Asia (43%), succeeded by Africa (31%), and America (28.4%) (Zhou and Lv, 2020). Another study found that a five-fold (3-17.1%) increase in CIP opposition was detected between 2000 to 2010 compared to other antibiotics studied (Fasugba et al., 2015). Other studies have recently shown the emergence of bacterial resistance to CIP, accounting for about 36.4%, and also noted that most strains of *E. coli* in particular showed resistance to CIP (Vol et al., 2022). A study done by Reis *et al.*, found that *E. coli* has the highest CIP resistance rate among bacteria that cause UTIs, with 36 % was found (Reis et al., 2016).

To treat infections caused by such strains, new antibiotics with novel modes of action are urgently needed. Though, all-embracing and difficult monitoring approvals have shifted the focus to improving the effectiveness of existing knockout medicines (Livermore, 2011) due to costly and lengthy processes of searching and developing of a new entities of antibiotics effective for resistant bacteria. Hence, nanotechnology is the first and recent focus areas that scientists are focusing on to combat such emerging resistant bacteria by improving the effectiveness of existing knockout drugs (Wu et al., 2022). Advances in nanotechnology are providing exciting ways to aid biofilm penetration, enhance drug entry into bacteria, and provide novel materials that synergize with unique functional properties (Pinto et al., 2019). A number of NPs have been mentioned to have significant anti-MDR bacterial strains action (Patrascu et al., 2015) including resistant *E. coli* (Caamano and Carrillo, 2016).

1.1.2. Nanotechnology

Nanotechnology encapsulates a progressive track for mechanical development that stresses over the administration of material at the nanometer scale (Malik et al., 2023). Nanotechnology unambiguously denotes any knowledge of the nanoscale that has several real-world applications (Biswas et al., 2023). According to fact, "nanotechnology" refers to the expansion and use of

materials at length with a range of scales (1-150nm) from single submicron-sized molecules or atoms and moreover the integration of the resulting nanomaterials into larger systems (Kumar et al., 2023).

The study of nanotechnology has advanced and has the possibility to transform many different ideas, including those in the realm of science. These systems have distinctive physical, electrical, and optical characteristics that make them intriguing in a range of fields, from biology to materials research (Wang, 2023). Nanotechnology is regarded as a recent and rapidly expanding breakthrough in the pharmaceutical and medical fields. As a targeted medicine conveyance method using a material with a magnetic response, particularly metallic and metallic oxide variations, nanotechnology is one of the most significant fields in nano carrier technology (Karpagavinayagam and Vedhi, 2019).

Pharmaceutical industry encompassing nanotechnology opens up different opportunities for creating unique preparations using a variety of NP types, taking into account their various sizes and shapes as well as their varied antibacterial capabilities. Since they can operate as medication delivery systems or as standalone direct targets of bacteria, these NPs may offer a promising resolution (Fatima et al., 2021).

1.1.2.1. Nanoparticles (NPs)

NPs are defined by the European Commission as solid particles, which comprise materials in which a minimum of half of the particles are equivalent to or less than 100 nm (Linsinger et al., 2012). They frequently exhibit novel and unique electrical, optics, attracting, natural, and chemical characteristics as well (Yu et al., 2021). Furthermore, NPs can be made of a number of materials, including composite polymers, semiconductors, metals, and even lipids and proteins, and they can have many shapes, such as spheres, rods, or tubes. There is a lot of interest in using NPs to develop new materials with unusual and innovative properties because of their various properties (Navya et al., 2019).

Due to the occurrence of particular and manageable features that differ from those observed on the macroscopic dimensions materials, NPs with 1 to 100 nm size range are able to perform a variety of unique applications. With regard to increased efficacy and fewer adverse medication reactions, NPs as drug delivery methods provide a number of benefits (Bayda et al., 2020). In the

realm of directed nutrients, minerals, chemicals, or medicine carriage systems, it is worth more credit (Ali et al., 2016).

In order to upsurge the efficacy of NPs against harmful MDR bacterial strains, new techniques like surface modification of NPs are being investigated (Satar et al., 2016). The two key modifications in NPs' features that allow them for using in such novel applications are due to the impacts of the surface, or the reduced size effect; for example, when particle size is lowered, a greater percentage of atoms are located at the surface, and modification of quantum confinement in the electronic structure initiated (Kulkarni et al., 2020).

1.1.2.2. Synthesis of NPs

The top-down or dispersion strategy and the bottom-up or condensation approach are the two main methods used to synthesize NPs. In the bottom-up method, the NPs are built up as a result of the interaction of molecule by molecule or atom by atom, as opposed to the top-down approach, where the NPs are generated via size reduction (Sreekanth et al., 2018) and can be produced using a diversity of methods, including green, chemical, and physical synthesis methods (Balamurugan et al., 2014, Dowlath et al., 2021).

Reduction/oxidation is the primary reaction that takes place during the bio fabrication of NPs, which is a type of bottom-up methodology (Maity et al., 2023). The reduction of salts into their particular NPs is often carried out by microbial enzymes or plant phytochemicals with anti-oxidant or reducing capabilities. In general, the biosynthesis approach is a low-cost option, biocompatible, and pharmaceutically compatible route that employs green chemicals (Aboyewa et al., 2021).

Reduction, growth, and termination are the three key phases of the green processing of NPs. Metal ions are oxidized/reduced by phytochemicals in the extract during the reduction phase. This stage is brought on by the metallic ions' electrostatic power of attraction to the phytochemicals. The termination phase, which involves the reduction of any leftover metal ions, follows the development stage, during which metal atoms are severed from their metal precursors and gather to form NPs (Selvaraj et al., 2022).

1.1.2.3. Iron oxide nanoparticles (IONPs)

The most prevalent elements on Earth and the fourth-most prevalent metal in the crust is iron (Pushcharovsky, 2019). One of the important microelements in living systems is iron. It performs a number of crucial tasks, including being a cofactor for a number of enzymes (such as catalase) and transport proteins (such as hemoglobin), as well as electron transport chain (ETC) proteins and being essential for repair of the DNA (Kronstad and Caza, 2013). In the laboratory, iron oxides are easily manufactured and are a common substance that is found throughout nature (Li et al., 2023).

Because of their biological suitability, chemical stability, and attractive behavior, magnetic nanoparticles (MNPs), one type of NP, have been the subject of considerable research in the biomedical arena. IONPs are a form of MNP that is readily available, adaptable, biocompatible, and biodegradable (Niculescu et al., 2022), and used as a good drug delivery strategy for resistant microorganisms in the industry of the pharmaceuticals (Mahdavi et al., 2013).

IONPs come in the variability of polymorphs and there are various sorts of them. The most popular ones are magnetite (Fe_3O_4), maghemite (γ-Fe_2O_3), and hematite (α-Fe_2O_3) (Khalil et al., 2017). Hematite, one of them, has a hexagonal centered, geometrically rhombohedral with a densely packed oxygen lattice (Zboril et al., 2002) making it a more chemically and thermodynamically stable candidate. Heat treatment, however, enhances crystallinity, changes the color, and encourages particle growth (Shen et al., 2014). In the occurrence of oxygen and a certain heat, the thermodynamically unstable magnetite and maghemite oxidize to form hematite. The generation of Fe_3O_4 at roughly 400°C and Fe_2O_3 at 800°C from the produced IONPs sample required calcination, as validated by (Justus et al., 2019). Additionally, according to Archana et al., the synthetic IONPs that were calcined at 700°C showed hematite peaks with high crystallinity (Archana et al., 2021).

IONPs have a relative advantage in terms of its toxicity, and amenability to human physiology after its duration of action in the body because our body uses it in different physiological hemostasis like in hemoglobin after the end of its activity in the body (Iv et al., 2015) A further study revealed that ferritin and transferrin played a part in the bio distribution of degradation products and also the *in vivo* biodegradation of IONPs (Arami et al., 2015, Feng et al., 2018).

Normal levels of hemoglobin protein, myoglobin, transferrin, and ferritin are found in the human body at 65%, 4%, 0.1%, and 15%–30%, respectively. It is thought that IONPs degrade at a molecular level in a manner similar to ferritins (Edge et al., 2016). Aside from this, the sectors of water treatment and cosmetics are also widely known for using α-Fe_2O_3 NPs. Because it is stable and inert, less toxic, and biocompatible, α-Fe_2O_3 is an excellent material for drug conveyance, imaging, directing treatment, cell conjugates, and as a benchmark for assessing metallic oxides characteristics from other metals (Ali et al., 2018).

1.1.2.4. Antibacterial application of IONPs

An imperative global public health concern now is the clinical management of pathogenic infections. The only available therapeutic option nowadays is an antibiotic, regardless of the fact that a misuse of antibiotics has headed to drug opposition in many cases and an increase in accident rates during anti-infection therapies (Manjusha et al., 2023). Because of the development of various biological and pharmaceutical delivery applications, scientists from all over the world have grown interested in nanotechnology (Edis et al., 2021).

Because of their remarkable lesser size and super paramagnetic activity, powerful noninvasive NPs known as super paramagnetic IONPs are widely used in nanomedicine uses like targeted delivery of antibiotics, and moreover magnetic resonance imaging hyperthermia (Bakhtiary et al., 2016).

Targeted medication delivery is one of the biomedical applications for which IONPs have been studied (Senapati et al., 2018), and killing with antibacterial effect (Teow et al., 2018). IONPs' benefits, including their low cost of production, excellent physiochemical characteristics and stability, biocompatibility, and biodegradability, make them ideal for both cancer therapy and other medical applications (Mühlberger et al., 2019).

Green synthetic IONPs with various surface functionalization are a promising area in the advance of novel antibiotics with a newer mechanism of action by loading the medication that is having trouble combating the drug-resistant bacterium (Arakha et al., 2015). Due to mimicking the easy passage of the loaded antibiotics into the bacterial cell due to its nano size carrier system, IONPs loaded with resisted antibiotics as a nanometric carrier (Arakha et al., 2015) is a promising and emerging technology to reverse the bacterial resistance of the antibiotics (Arias et

al., 2018). The IONPs' synergistic effect is not all that they have to offer (Dreaden et al., 2012, Pugazhendhi et al., 2018).

Vihodceva *et al*. observed that uncoated NPs which have positively charge inhibite the development of *E. coli* within 30 minutes of exposure at 100 mg/L concentration; the inhibitory properties of NPs were obvious at 10 mg/L, and the 24 h minimum concentration having bactericidal effect was 100 mg/L. As a result, the influence of NPs grew with time (Vihodceva et al., 2021). IONPs were reported to have inhibited *E. coli* in other studies as well. The IONPs did not demonstrate any significant changes in the dose of 12.5 mg/mL based on antibacterial characteristics, however with substantial increase in dosage there was increased in the inhibition (Rafi et al., 2015). Another research found that iron NPs had a good ZOI in mm (20.45 ± 1.66) on *E. coli* (Tyagi et al., 2021). Baniasadi et al. likewise came to the conclusion that IONPs had an extensive variety of effects at extremely low concentrations against bacteria that had a substantial amount of antibiotic resistance (Baniasadi et al., 2020).

1.1.2.5. CIP loaded NPs as bacterial resistant reversal

New tactics and defensive mechanisms against MDR pathogenic organisms have been proposed, such as the use of nanostructures with antibacterial activity or nanocarriers that can modify antibiotic transport and administration (Terreni et al., 2021). The rigorous use of nanomaterials has provided a viable strategy for improving the present approach to treating microbial illness in order to prevent antibiotic resistance (Hochvaldová et al., 2022). Bacterial Biofilms are one type of the primary sources of biocide conflict. Metallic NPs, such as zinc oxide, iron oxide, and silver NPs, have been used successfully to treat infections caused by biofilms as a result of their antibacterial qualities (Mubeen et al., 2021).

In order to deliver bioactive compounds, metal-based NPs are utilized. These NPs are well-known to having nonspecific methods of noxiousness toward bacteria it makes it more difficult for bacteria to strengthen resistance while NPs widening the antibacterial spectrum of the medicine. Combination treatment with resistant antibiotics and metal-based NPs might be one approach to combating existing bacterial drug resistance (Aruna et al., 2023).

There is various metal oxide and metal NPs with CIP loaded into them that have more bacterial inhibitory activity than both CIP and the bare nanoparticles (Maleki Dizaj et al., 2017, Mohsen et

al., 2020, Nawaz et al., 2021b). A meaningful increase in solubility, pharmacokinetics, bioavailability, and strong antibacterial activity were observed after CIP capping with metallic NPs such as silver and gold NPs in optimal conditions (Nisar et al., 2016). CIP-AuNPs are gold nanoparticles, and they are among the majority of recently reported nano carriers for CIP (Tom et al., 2004), CIP-loaded nano composites (Topal et al., 2018), poly Lactic-Co-Glycolic Acid (PLGA)–chitosan-based CIP (Arafa et al., 2020), CIP containing polymer-based nano fibers (scaffolds) (Albuquerque et al., 2015), and CIP-loaded carbon nanotubes, single-walled (Assali et al., 2017) have promising worth and new possibilities in regards to handling such resistant microbes which are the ongoing consuming issue because of their hardships in treating them with at present accessible medications (Maleki Dizaj et al., 2017).

Already, a number of goods use metal oxide nanoparticles (NPs) as an antibacterial ingredient. The ability to pinpoint precise places is improved by metal oxides having magnetic drug delivery capabilities, such as iron oxide, which also lowers the concentration of non-target drugs (Stanicki et al., 2022). According to Kooti et al., CIP-loaded cobalt ferrite ($CoFe_2O_4$) which target the bacteria using magnetic field, caused the inhibition zone multiply by two and also releasing drugs in a regulated manner (Kooti et al., 2018). According to research done by Sirivisoot and Harrison, PCL-CIP-maghemite and PCL-CIP-hematite both more effectively subdued bacterial proliferation in the presence of a attractive field after 2 to 5 days of culture (Sirivisoot and Harrison, 2015). Additionally, there are many steel and metallic oxide NPs loaded with CIP that have greater bacterial inhibitory activity than CIP and the bare NPs (Maleki Dizaj et al., 2017, Mohsen et al., 2020, Nawaz et al., 2021b)

1.1.3. Banana plant (*Musa spp*.)

The *Musaceae family*, which includes the three genera *Musa, Musella, and Ensete*, includes the herbaceous banana plant (Fu et al., 2022). The primary species that produces edible bananas are *Musa spp.* (Sardos et al., 2016). Banana plants are farmed principally because of their fruit and, to a lesser extent, for use in the production of natural fibers and wine (Amini et al., 2019). Typically elliptical in shape, bananas' fruits come with creamy "pre-packed", solid flesh encased in a dense peal that is a rich source of flavonoids, polyphenols, and tannins (Al-Mqbali and Hossain, 2019).

The banana, a fruit of tropical, is grownup in over 130 countries. Bananas (*Musa spp*.) are the most important staple and commercial crop, with an annual production worldwide of 113.9 million tons (Tong et al., 2023). It ranks fourth in terms of food crop significance, behind rice, wheat, and corn, and is the world's second most produced fruit. It accounting for about 16 percepts of all fruits produced globally. It is more easily digested than numerous other fruit varieties and is quite nutritious (Kuyu and Tola, 2018). Africa, Latin America, the Caribbean, Asia, and the Pacific are merely a few examples of the many nations where it is grown, with the majority of them being in the warm, humid, and rainy tropical regions of the planet. Over 70 million Africans depend on bananas for 25% of their calorie intake (Boris et al., 2023). In the tropical nations like Ethiopia, where there is a lot of fertile land, banana farming is feasible (Dagnew et al., 2021).

According to CSA 2014, in Ethiopia, bananas are the main fruit that is most frequently grownup and utilized, accounting for around 59.64% (53,956.13 hectares) in terms of the entire fruit space and approximately 68% (478,251.04 tons) of the entire fruit produced. In contrast, according to the CSA (2014), around 68.72% (37,076.83 hectares) of the land is planted with bananas. It is grown in a variety of locations where the growth environment is favorable. It is of immense socioeconomic importance, particularly in the south and southwest of the country, and considerably contributes to the general wellbeing of rural areas, including security of the food, income generation, and job development (Debebe and Dagne, 2018).

Due to the chemicals found in the fruit peel of bananas, which are employed in the process of NP synthesis, as a stabilizing and reducing component, bananas are a possible source for green synthesis of NPs. The plant is more appropriate for this unique use since it can be grown most easily both locally and globally, and there is a strong likelihood that its waste products will be used (Ibrahim et al., 2017).

1.1.3.1. *Banana peels extract*

The primary source of banana waste is the peels, which make about 40% of the weight of the fruit of bananas. Approximately trash totaled 114.08 million tons in weight, from banana production are created globally, which causes issues with the environment such excessive greenhouse gas emissions (Alzate et al., 2021). Nearly 60% of the biomass from bananas is thrown away after harvest. Regarding the accessibility and affordability of the excipients utilized

in the NP synthesis, recycling the bio-waste has advantages. Additionally, it aids in the mitigation of environmental pollution brought on by the emission of gases during their various mechanisms of deterioration (Padam et al., 2014).

Peels from fruits have been discovered to include a range of useful second-generation metabolites, such as polysaccharides, different phenolic compound, flavonoids, and other substances. Because these components may be sources of prospective prebiotics and antioxidants that are advantageous to both human health and food, and pharmaceutical sectors, the recovery of these highly valuable chemicals could be commercially appealing (Chamorro et al., 2022). As a result of containing phenolic 18.21 to 35.06 mg Gallic acid/g and flavonoid 196.1 $\pm$ 6.7 mg/g of peel extract, banana peel extract, which contains such important chemicals, is one of the stabilizing and reducing agents in the creation of IONPs (Anal et al., 2014).

In addition to being one of the primary ingredients in the IONP green fabrication as a stabilizing and reducing agent, banana peel extract also has antibacterial action against *E. coli* as a synergistic effect for the formulation. According to a research on the evaluation of the antibacterial properties of banana peel extract, *E. coli* growth was inhibited with an inhibitory zone that varied from 9.2 to 13.37 mm at a dose of 20% and from 10.03 to 13.97 mm with a 50% of the extract contents (Rita et al., 2020). Additionally, there was a strong link between the flavonoid and phenolic content alongside its antimicrobial action (Rita et al., 2020, Susanah et al., 2018).

Hence, this research aims to synthesize and evaluate IONPs synthesized making use of banana peel essence as an agent that reduces and becomes stable for CIP delivery against resistant *E. coli*.

1.2. Statements of the problem

Currently in the world, one of the major concerns and rapidly growing problem is antimicrobial drug resistance. It leads the world in to unexpected whelms unless other ways a novel method is developed to stop or reduce such trebling situation. As a result, nowadays, the world gives a great emphasis on searching for a novel strategy to overcome the burden of antibacterial drug resistance using the available drug by modifying their delivery through nanotechnology (Malhotra et al., 2020).

The majority of IONPs are produced through physical and chemical processes (Ali et al., 2016). However, these approaches are expensive, lengthy, and unsafe for any biomedical use (Ali et al., 2016). Physical procedures are less efficient, expensive, expose workers to radiation, and need high temperatures for synthesizing IONPs, as opposed to chemical approaches that utilize hazardous precursors. They typically create NPs with poorer features than green synthesis methods, offer a significant environmental risk, consume a lot of energy, pose a risk to one's health, and not biocompatible (Dowlath et al., 2021).

The earth is now warming faster than at any other moment in recorded history. Weather conditions are changing as a consequence of warming temperatures, which is also hurtful for the natural life. Greenhouse gas emissions are a major contributor to global warming. There is a significant amount of banana fruit waste product that contributes to environmental degradation and global warming due to large emissions of methane (CH4), nitrous oxide (N2O), and carbon dioxide (CO2). These emissions cause catastrophic climatic changes, such as floods, droughts, and heat waves. These provide several threats to both people and all other kinds of Earth's life. The enormous amount of banana peel trash produced daily by the fruit and juice industries points to a potential bio-resource that might play a significant influence in reducing environmental impact owing to greenhouse gas emissions (Alzate et al., 2021, Sial et al., 2019).

Numerous studies revealed that IONPs have good at *in vivo* and *in vitro* performance of biocompatibility and are relatively safe (Hanini et al., 2011, Yiu et al., 2012), which, in terms of quality, set IONPs apart from other metallic NPs, such as those with significant cytotoxicity like zinc oxide, silver, and gold (Gong et al., 2017).

1.3. Significance of the study

The significance of this research is in examining of one of the promising and newly developed methods for reducing drug resistance in bacteria by using nano sized carriers that make it easier for the drug to enter the bacteria and IONPs' antimicrobial activity as a synergistic method against CIP resistant *E. coli*.

Both the antibacterial action and biological suitability IONPs makes an interesting contender for the position of a new-generation antimicrobial researcher. IONP is the most preferred nanomaterial in the field of medical sciences because of their low toxicity and unpaid

physiochemical qualities such as super paramagnetic, aqueous solutions stability, biocompatibility, and the iron metabolism pathways efficiently remove it from the human body.

Focusing on banana peel waste which is richest in reducing and stabilizing secondary metabolites conceding with its pronounced antibacterial activity will have multiple significance regarding availability, cost-effectiveness, pollution reduction, and development of effective IONPs.

The green synthesis of IONPs using banana peels extracts offers a good alternative with the desired characteristics, eco-friendly, biocompatible, economical, rapid and less toxic than the other methods of synthesis for CIP delivery against CIP-resistant *E. coli*, which has a great significance on reducing the currently emerging antimicrobial resistant bacteria.

This study can also be used as a baseline data for further investigation and development of the formulation.

2. Research questions

- How much is the yield of IONPs synthesized using banana peels extract?
- What is the encapsulating and CIP loading efficacy of IONPs synthesized using banana peels extract?
- What is the CIP release pattern of CIP-IONPs at different simulation fluid?
- What is the effect of CIP-IONPs on CIP resistant *E. coli*?

3. Objectives of the study

3.1. General objective

- To synthesize IONPs using Banana (*Musa spp*) peals extract for delivery of CIP against resistant *E. coli*.

3.2. Specific objectives

- To synthesize IONPs using Banana (*Musa spp*) peals extract as a stabilizing and reducing agent,
- To optimize operational factors for IONPs synthesis,
- To investigate the drug loading and drug encapsulation efficiency of IONPs,
- To characterize the physicochemical properties of IONPs and CIP-IONPs,
- To determine the *in vitro* drug release profiles of CIP-IONPs and
- To evaluate the *in vitro* effect of CIP-IONPs against CIP resistant *E. coli* as compared with CIP and IONPs.

4. Methods and Materials

4.1. Materials collection

CIP HCl (Batch No: A2023-090, Mfg. date: 13/03/2023, Exp. date: 12/03/2027, 99.9%, China) was kindly donated by Humanwell Pharmaceutical Industry Ethiopia. Clinical isolates of CIP-resistant *E. coli* were acquired from the microbial stock of the Medical Laboratory Department of the College of Medicine and Health Sciences, Debre Berhan University. Banana peels (Musa spp.) were gathered from several juice houses in Debre Berhan Town, North Shewa Zone, Amhara Region. Other materials and chemicals that were used in the study include acetic acid (99.7% GJ chemical), ethanol (70 %, Dallul Pharmaceuticals PLC), chloroform AR (Reagent Chemical Services Ltd., UK), sulfuric acid (98%, Loba Chemie Pvt. Ltd., India), ammonium hydroxide (99% Xingtai Weijiate Biotechnology Co., LTD), hydrochloric acid (35.4%, Loba Chemie Pvt. Ltd.,India), potassium iodide (99-100.5%, Loba Chemie Pvt. Ltd., India), ferric chloride (99%, Loba Chemie Pvt. Ltd., India), iodine (Reagent Chemical Services Ltd., UK), gelatin powder (Blulux Laboratories Ltd., India), sodium hydroxide (99.8% Norbright, China), potassium chloride (99% BDH Limited Poole, England), potassium dihydrogen orthophosphate (99%, TITAN BIOTECH LTD., India), distilled water, Whatman No.1 filter paper, dialysis Sack (a flat width of 35 mm on average, and 12 kDa molecular weight cutoff, SIGMA-ALDRICH, USA), Müller-Hinton agar (Sisco Research Laboratories Pvt. Ltd.) and other common laboratory equipment and supplies for this work were used.

4.2. Preparation of banana (*Musa Spp*.) peel extract

The peels of bananas were cleaned with distilled water three times to remove external dirt and stored at ambient temperature for a period of time till dry. Then, I chopped it into a small piece with a stainless-steel knife and finely chopped it with an electronic blender. (Vitamix, model: 59326) then crushed to a fine powder with a mortar and pestle. In a conical flask with the mouth covered with aluminum foil, the powder sample was soaked in 70% ethanol in a ratio of 1:3, peels powder to solvent. The macerate was kept at room temperature for three days (Chaudhry et al., 2022). The extract was filtered twice through Whatman filter paper No. 1 to exclude insoluble components. The resulting filtrate was stored in aluminum foil sealed container at 4°C.

4.3. Phytochemical analysis of banana peel extract

Banana fruits cover extract samples were tested for the presence of several common secondary metabolites using methods reported elsewhere.

4.3.1. Flavonoids

Two magnesium ribbons and three drops of concentrated hydrochloric acid were combined with 2 ml of banana peel extract within a test tube (Roghini and Vijayalakshmi, 2018).

4.3.2. Tannin

2 ml of 1% gelatin solution containing sodium chloride added to 5 ml of banana peel extract., (Roghini and Vijayalakshmi, 2018).

4.3.3. Saponins

Two milliliters of water were blended with 5 milliliters of extract from banana peels. (Sonam et al., 2017)

4.3.4. Anthraquinons

Two milliliters of banana peel extract was added to two milliliters of ammonium hydroxide solution (Shaikh and Patil, 2020).

4.3.5. Terpenoids

Two milliliters of banana peel extract were combined with two milliliters of chloroform and three milliliters of sulfuric acid (Nasrabadi et al., 2013).

4.3.6. Phenols

2 milliliters of the extract of banana peel was mixed with 3 drops of 0.1% ferric chloride solution (Sonam et al., 2017)

4.3.7. Glycosides

A couple of milliliters of ferric chloride solution were mixed with 4 ml of banana peels extracts. They were then immersed in water boiled for around 5 minutes. The mixture cooled down and benzene was added. It was then divided into two test tubes and cured with ammonia (Kumar et al., 2011).

4.3.8. Steroids

Two milliliters of banana peel extract were mixed with two milliliters of chloroform and acetic acid two milliliters, and finally, one milliliter sulfuric acid concentrated was mixed to the mixture (Sumathy et al., 2011).

4.3.9. Alkaloids

2 milliliters of banana peel extract treated with 4 drops of Wagner's reagent (Shaikh and Patil, 2020).

4.4. Synthesis of IONPs using banana peels extract

For the fabrication of the α-Fe_2O_3 NPs, ferric chloride hexahydrate (FeCl3.6H2O) was employed as a precursor. Banana peel extract and 0.5M concentration of $FeC1_3.6H_2O$ solution were combined in a ratio of 1:2 at normal temperatures in the room. After that, 1M NaOH was added until the pH reached 12. The resultant mixture was stirred at 1000 rpm with a magnetic stirrer for 1 hour, and the color gradually changed to brown. The brown-colored colloidal suspension was centrifuged using a centrifuge (Beckman Coulter Allegra 64R, USA) at 10,000 rpm for 20 minutes, rinsed three times with ethanol, followed by distilled water, then dried in an oven (Quincy Lab, 20GC) at 80^0c overnight. Finally, the formed IONPs were calcined at 700^0c for 2 hours using a furnace (Lss Ethiopia, EDS-MTLE-11467) that gives a red colored hematite NPs and kept in an airtight container for next use and characterizations (Bibi et al., 2019).

4.5. Optimization of physicochemical parameters for IONPs Synthesis

IONPs' distinct qualities, such as magnetic activity and antibacterial activity, depend on their shape and size (Chen et al., 2018, Huang et al., 2015), This has driven many studies to create size-controlled syntheses of IONPs (Xie et al., 2018). In previous studies, that fabrication factors for example, precursor concentration and extract-to-precursor ratio (Dehsari et al., 2017), pH (Andrade et al., 2010), reaction time (Kumar et al., 2013), reaction temperature (Liu et al., 2020a), plus annealing temperature (Chomchoey et al., 2018), influence the growth of NP crystallite size (Dharr et al., 2020). Therefore, the current study was conducted according to the procedure described by (Bibi et al., 2019). The optimization parameters shown in Table 1 were used as factors to identify the optimal parameters for the synthesis of IONPs by changing one factor and keeping the other constant. The first optimal factor identified was used to optimize the

other factors following this method (one factor at a time). The % yield value (Equation 1) and the size of IONPs were considered dependent variables and were examined using an analytical balance (Aarson, Chandigarh, India) and a particle size analyzer known as 90-plus (Brookhaven Instruments Corporation, USA), respectively. A parameter gave a greater % yield value within an acceptable size range of the NPs approximately 1 nm to 150 nm (Kush et al., 2021) was selected as the optimal value for the synthesis of IONPs.

Table 1: The optimization parameters and their values used for optimal synthesis of IONPs using banana peels extract.

	Parameters				
	Concentration of the precursor	**Banana peels extract to precursor ratio**	**pH of the media**	**Temperature of the media in ^{0}C**	**Reaction time in hour**
Values	0.1M	3:1	1.2	Room	0.5
	0.25M	2:1	2	40	1
	0.5M	1:1	4	60	2
	0.75M	1:2	6	80	3
	1M	1:3	8.5	100	4
			10		
			12		
			14		

$$\text{Yield value (\%)} = \frac{\text{Weight of IONPs synthesiszed}}{\text{Weight of precursor(FeCl3.6H2O) used}} \times 100 \qquad (1)$$

4.6. Optimization of parameters for preparation of CIP-IONPs

The drug loading of NPs was affected by a variety of processing parameters, including reaction time and drug concentration. In this study, the reaction time and contents of the drug were optimized. The λ_{max} and calibration curves of CIP were determined using standard CIP solutions of 2 µg/ml, 3 µg/ml, 4 µg/ml, 5 µg/ml, and 6 µg/ml. For the single-factor method, reaction periods of 0.5, 1, 2, and 4 hours and drug concentrations of 1.5, 5, 7.5, 10, 12.5, and 15 mM were used as optimization factor points, (Nawaz et al., 2021b, Soliman et al., 2022) using a UV-vis to ascertain CIP content in the supernatant of drug NP mixtures which were run for a specified reaction time.

4.7. Preparation of ciprofloxacin loaded IONPs (CIP-IONPs)

The method for loading CIP to IONPs was adopted from (Nawaz et al., 2021b). CIP was loaded on IONPs, by mixing 2.5 mL of 10mM concentrations of CIP solution with 1mg/ml of 10 mL IONPs suspension for 1hour with magnetic stirrer at 100rpm. The resulting mixture was centrifuged for 20 minutes at 10,000 rotations per minute to separate the CIP-IONPs. It was rinsed three times using distilled water for removing the unloaded drug from the CIP-IONPs. CIP-IONPs was dried at the temperature of the room and kept in a tightly sealed container for further characterization and application.

4.8. Encapsulation Efficiency and Drug Loading Capacity

Equations (2) and (3) were used to calculate the CIP load capability and encapsulating performance of IONP (Nawaz et al., 2021b).

$$\text{Loading capacity (\%)} = \frac{\text{The CIP weight in CIP– IONPs}}{\text{The weight of CIP– IONPs}} \times 100 \qquad (2)$$

$$\text{Encapsulation effectiveness (\%)} = \frac{\text{Total added CIP} - \text{Free CIP}}{\text{Total added CIP}} \times 100 \qquad (3)$$

4.9. Characterization of IONPs and CIP-IONPs

The synthesized IONPs and CIP-IONPs were characterized using various procedures and instruments toward confirm their formations besides study their physical, optical, and thermal properties (Al-Hakkani et al., 2021).

4.9.1. Analysis of dynamic light scattering (DLS)

DLS examination was performed utilizing a 90 plus particle size analyzer (Brookhaven Instruments Partnership, USA) to determine the hydrodynamic dimension for both IONP synthesis optimization and IONP and CIP-IONP portrayal and polydispersity (PDI) record assurance.

To avoid the interference of large particles during the measurement, a 0.22 μm syringe filter unit was used for filtration of both an aqueous suspension of CIP-IONPs and IONPs, which were sonicated for 5 min with an intelligent ultrasonic processor (SJIA-250W, Ningbo Yinzhou Sjia Lab Equipment Co. LTD, China) before determining the size and size distribution.

4.9.2. UV–Visible spectrophotometry investigation

Their respective absorbance of the produced IONPs and CIP-IONPs were examined by scanning through 200 to 800 nm using an ultraviolet and visible absorption spectrophotometer (ThermoFisher, Evolution 201, China).

4.9.3. Fourier transform-infra red (FTIR) spectroscopy exploration

To conclude the functional groups involved from extract of the banana peel for the formation of NPs and to identify the functional groups that exist in the synthesized NPs and drug-conjugated NPs the FTIR spectra of the peel extract, IONPs, CIP, and CIP-IONPs were measured at the 4000 to 400 cm^{-1} range, employing the KBr pellet approach on FTIR spectrophotometer (ThermoFisher, Nicolet iS5, China)..

4.9.4. Powder X-ray diffraction (XRD) examination

To determine crystal structure, average crystalline size, and composition of IONPs (phase purity), Powder X-ray diffraction examination was performed. The XRD pattern of created IONPs was determined by X-ray diffractometer (XRD-7000 X-RAY DIFFRACTOMETER, SHIMADZU Corporation, (Japan)) operating at a 40 kV voltage and a 30 mA current with a Cu

target in a continuous scanning range between 10 and 80 degrees of 2θ angel and with scanning speed of 3 degrees per minute and sampling pitch of 0.0200 degrees. The crystallite size of the NPs was calculated using the Debye-Scherrer formula (Equation 4).

$$D = \frac{0.9\lambda}{(\beta \cos\theta)} \qquad (4)$$

Where, D is the mean size of the particle, λ is the wavelength of X-ray; β is full width at half maximum intensity and θ is the diffraction (Bragg) angle (Selvanayaki et al., 2022).

4.9.5. Scanning electron microscopic (SEM) analysis

SEM (High-vac. SED PC-std. JCM-6000Plus) was used to ascertain the shape, size, and surface roughness of the produced IONPs.

4.9.6. Thermal analysis

Differential Thermal Gravimetry, (DTG - 60H), SHIMADZU Corporation, Japan), was used for the thermal analysis, which includes TGA and DTA for the measurement of weight loss, purity, decomposition, and phase change with regard to temperature (Naz et al., 2019b) in 15^0c/min temperature rate up to 800^0c.

4.10. Drug Release study

The λ_{max}, and calibration curve for each buffer solution used to release the study were determined using 2µm/ml, 3µm/ml, 4µm/ml, 5µm/ml, and 6µm/ml standard CIP solution using the respective buffers as a solvent. CIP release *in vitro* from the CIP-IONPs preparation was studied using the scheme described by (Zafar et al., 2021). Determination of the content CIP released using a UV-Vis was determined at 276, 271, and 270 nm in 1.2, 6.8, and 7.4 pH simulation fluid respectively. The study was taken over 24 hours. Briefly, a dialysis membrane sack with a molecular weight of 12 Kilo Daltons cut out that was soaked in respective simulation medium, which mimics different physiological pH using PBS for 24 hours at 37 $\pm$ 0.7°C and the bag was filled with 4ml of CIP-IONPs suspension which contained 2mg CIP-IONPs. After tying of both ends, the dialysis membrane bag was immersed into the receptor compartments containing 40 ml of PBS prepared for a particular pH simulation medium. The whole assembly was kept on 100 rpm shaker at 37$\pm$ 0.7°C using Shaking incubator (THZ-300, Shanghai Yiheng,

China). At predetermined intervals of time, aliquot (4 mL) were taken and replaced with fresh PBS adjusted for particular simulation medium, Equation 5 was used to compute the cumulative release of drugs (Zafar et al., 2021).

$$\text{Cumulative drug release (\%)} = \frac{\text{CIP liberated from CIP} - \text{IONPs at time t}}{\text{The total quantity of CIP loaded on IONPs}} \times 100 \quad (5)$$

4.11. *In Vitro* antibacterial susceptibility study of CIP-IONPs, IONPs and CIP

CIP resistant *E. coli* strain were isolated by conventional biochemical profile and an antimicrobial resistance study was carried according to Kirby-Bauer diffusion of the disk susceptibility test technique (Hudzicki, 2009). The bacteria were harvested using Mueller-Hinton agar for 24 hours. Mueller-Hinton agar plate was prepared and placed for 30 minutes in a laminar flow hood at ambient temperature for drying. The inoculum suspension comparable to turbidity of 0.5 McFarland was prepared. And it was inoculated on a Mueller-Hinton agar plate labeled for each standard sample solution using a sterile swab. The standard sample solution of 5µg/20µL CIP (CLSI, 2021); 15µg/20µL CIP-IONP, and 10µg/20µL IONP based on the loading capacity of the IONPs was impregnated on sterilized Whatman filter paper disc which was prepared by office puncher. This impregnated disc was placed on an inoculated Mueller-Hinton agar plate respective to their label and incubated at (37^0C ± 0.5) for 24 hours after inverting the plate upside down. Finally, a zone of restriction was determined using a ruler. CIP-IONPs, IONP, and free CIP antimicrobial properties were compared (Hudzicki, 2009).

4.12. Statistical analysis

Statistical data was evaluated using Origin Pro 2022 version of the software was 9.9.0.225 and ImageJ, Java 8.2 software. The results were displayed using graphs and tables.

5. Result and discussions

5.1. Qualitative phytochemical analysis

Qualitative screenings of phytochemicals in extracts of banana peel demonstrate the existence of diverse phytoconstituents, as shown in Table 2.

Table 2: Phytochemical screening of banana peel extracts

S/No	Phytochemicals	Indication	Result
1	Flavonoids	Pink or red color	Positive
2	Alkaloid	Brown/reddish precipitate	Positive
3	Tannin	White precipitate	Positive
4	Saponins	Foam produced persists for ten minutes	Negative
5	Phenols	Bluish-black color	Positive
6	Glycosides	Rose-pink color	Positive
7	Steroids	A Blue-greenish color	Positive
8	Terpenoids	Reddish brown color	Positive
9	Anthraquinons	Bright pink color	positive

Even though the synthetic mechanism of IONPs is not completely understood, terpenoids, flavonoids, various heterocycles, (Morales-Díaz et al., 2016) and polyphenols are directly engaged in the production (Wang et al., 2015) of iron oxides, zero-valent iron, and a combination of all IONPs (Kanagasubbulakshmi and Kadirvelu, 2017, Nwamezie, 2018, Saif et al., 2016), The presence of such phytochemicals and others like, tannins, glycosides and coumarins in banana peel extracts were also reported before (Zaini et al., 2022). Therefore, as these phytochemicals are in charge of the development of IONPs, their presence in extract of banana peel confirms the capability of the plant essences to produce the NPs.

5.2. Synthesis of IONPs using banana peels extract

5.2.1. Visual inspections

Visual observation of the color change during the synthesis is cited in various sources as the first qualitative investigation of the creation of IONPs (Asoufi et al., 2018, Naz et al., 2019a, Sundara Selvam et al., 2020). In this investigation, there was a hue change from black to brown,

suggesting the existence of IONPs (Figure 1) after drop wise mixing of the banana peels extract with precursor except in acidic pH (1, 2, 4, and 6), and in 3:1 extract to precursor ratio. The finding was in line with different reported literatures (Asoufi et al., 2018, Naz et al., 2019a, Sundara Selvam et al., 2020).

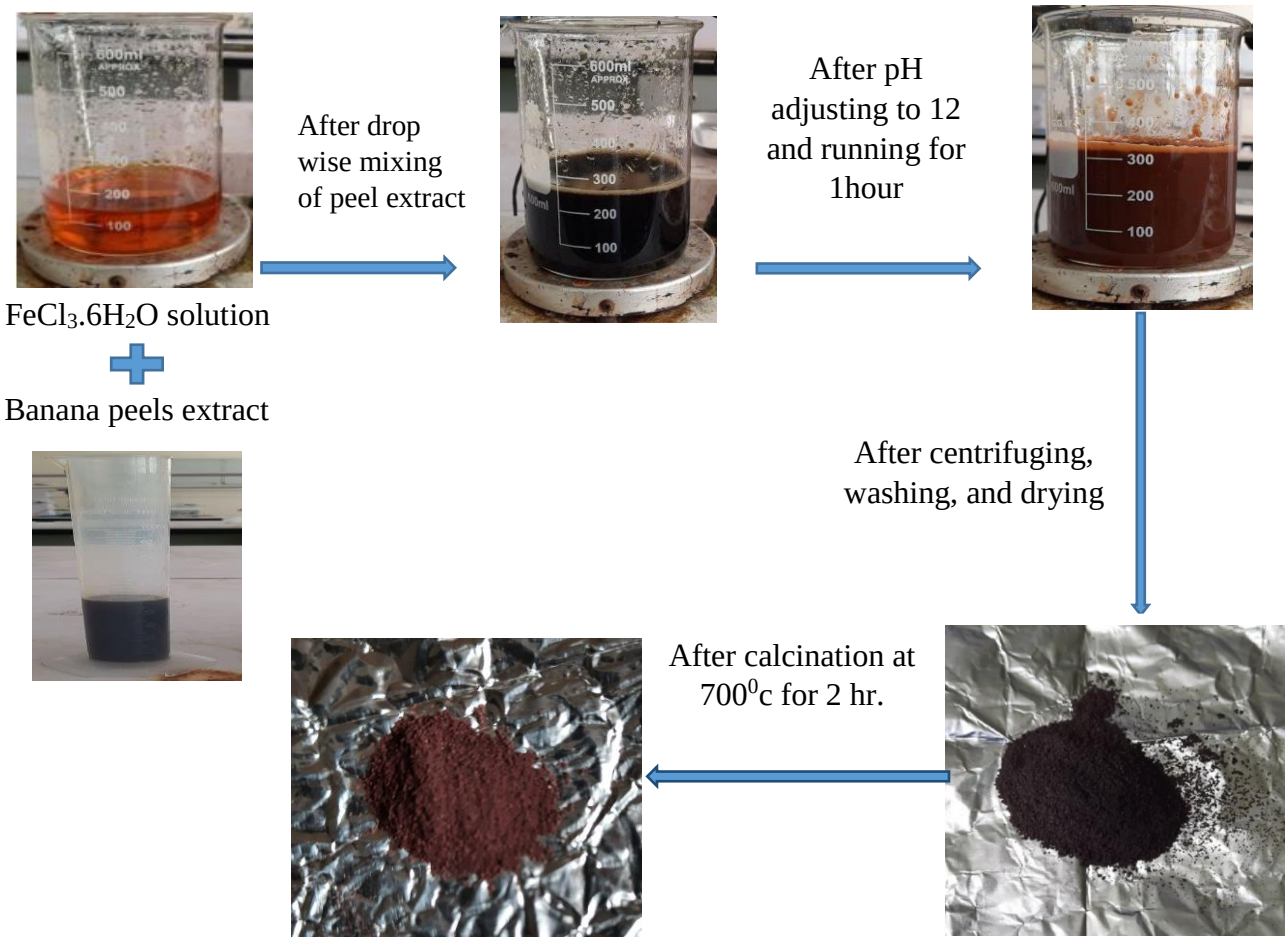

Figure 2: Schematic illustration of color change in synthesis of IONPs using banana peels extract.

5.2.2. Optimization of IONPs synthesis parameters

For the best creation of IONPs, the parameters of pH, extract to precursor ratio, and precursor concentration, temperature, and reaction durations were tuned.

5.2.2.1. Precursor concentration

One among the most elements influencing the size, quantity, and properties of synthesized NPs is the precursor's concentration. According to research by Kriedemann and Fester (2015), the average size of particles of the fabricated IONPs is 76.5% dependent on the precursor's content (Kriedemann and Fester, 2015). This investigation discovered that the size of produced IONPs were increased as the precursor's content was increased which is consistent with research done by (Dehsari et al., 2017) (Table 3). However, the % yield values were observed to increase from 0.245% to 6.91% while increasing the concentration of the precursor 0.1M to 0.5M, but it was decreased in farther increasing of the concentration from 0.5M to 1M (Table 3), this is consistent with a study done by (Erkakan et al., 2022). This study looked at; 0.5M concentration of precursor was selected for optimization of the next trials because it gave relatively the largest % yield value (6.91%) than other IONPs synthesized within acceptable particle size (109.5nm).

Table 3: Effective diameters and yield values of IONPs synthesized utilizing banana peels extract at different precursor concentration.

Independent variables					**Dependent variables**	
$FeCl_3.6H_2O$ Conc. In M	**Ratio P. Ext.: Precu.**	**pH**	**T^0 (^0C)**	**Reaction Time In hr**	**Yield value (%)**	**Effective Diameter (nm)**
0.1	2:1	8.5	Room	0.5	0.245	120.1
0.25	2:1	8.5	Room	0.5	0.74	122.6
0.5	**2:1**	**8.5**	**Room**	**0.5**	**6.91**	**109.5**
0.75	2:1	8.5	Room	0.5	2.7	125.8
1	2:1	8.5	Room	0.5	1.23	150.1

5.2.2.2. Extract to precursor ratio

The ratio of biocatalyst to precursor is supposed to be a crucial factor in defining the size and rate of NPs production (Jacob et al., 2019). One of the factors to determine the effective qualities of the particles, especially size, is the extract to precursor ratio (Aragaw et al., 2021), so in this research the extract to precursor ratio 3:1, 2:1, 1:1, 1:2, and 1:3 trials were done for finding the optimal ratio but 3:1 ratio did not give any measurable amount of the NPs for DLS analysis (Table 4). The trends of % yield values were similar to the precursor concentration in that the plant extract ratio decreased, the % yield value increased up to some instance after that it

was decreased. which corresponds to a study by Hong and Jiang that found that the yield values of the synthesis of NPs increased as the extract ratio climbed from 10% to 30%, but that the yield values fell as the extract ratio increased from 30% to 50% (Hong and Jiang, 2017). This may due to decreasing the plant extract leads to increasing in precursor concentration. In this research, an extract to precursor ratio of 1:2 gave the best result (25.98% and 102.6nm) and it was hired for the next optimization trials.

Table 4: Effective diameters and yield values of IONPs synthesized utilizing banana peels extract at different extract to precursor ratio.

Independent variables					**Dependent variables**	
$FeCl_3.6H_2O$ Conc. In M	**Ratio P. Ext.: Precu.**	**pH**	**T^0 (^0C)**	**Reaction Time In hr**	**Yield value (%)**	**Effective Diameter(nm)**
0.5	2:1	8.5	Room	0.5	6.91	109.5
0.5	1:1	8.5	Room	0.5	19	130.8
0.5	**1:2**	**8.5**	**Room**	**0.5**	**25.98**	**102.6**
0.5	1:3	8.5	Room	0.5	8.4	134.2

5.2.2.3. pH

The reaction's pH level also played a crucial part in the production of NPs. pH, like temperature, also controls how nucleation centers occur. An upsurge in many nucleation centers happened due to alkaline environment as the pH rises. The likelihood of accessible functional groups was made more likely by pH, which promoted the fabrication of metallic NPs (Samuel et al., 2022). pH has been shown a substantial impact in determining the dimension and morphology of the particles (Karade et al., 2018). Without pH adjustment, it is impossible to create NPs with a precise morphology and size. Various plant extracts have diverse chemical compositions, and it has happened that different pH values cause the creation of NPs (Soni and Prakash, 2011). In this study, different pH values were taken into consideration for the optimal synthesis of IONPs using banana peels extract starting from pH 1 to 14. But there were no formed NPs at pH 1, 2, 4, and 6 whereas pH values of 8.5, 10, 12, and 14 gave NPs (Table 5). These NPs forming pH values showed comparable results for the % yield value and different particle sizes indicating that pH has a strong influence on particle size determination rather than yield value. A pH of 12

gave relatively the largest % yield value (27.40%) and acceptable particle sizes (89.1 nm) was selected for the next optimization process.

Table 5: Effective diameters and yield values of IONPs synthesized utilizing banana peels extract at different pH

Independent variables					**Dependent variables**	
$FeCl_3.6H_2O$ Conc. In M	**Ratio P. Ext.: Precu.**	**pH**	**T^0 (^0C)**	**Reaction Time In hr**	**Yield value (%)**	**Effective Diameter(nm)**
0.5	1:2	8.5	Room	0.5	25.98	102.6
0.5	1:2	10	Room	0.5	25.18	121.1
0.5	**1:2**	**12**	**Room**	**0.5**	**27.40**	**89.1**
0.5	1:2	14	Room	0.5	24.44	274.2

5.2.2.4. Temperature

The consequence of temperature on NPs synthesis was widely examined and recognized as most influential factors that meaningfully influence NP synthesis rate, dimension, and form (Fleitas-Salazar et al., 2017). In this research, the particles size was increased while increasing the temperature (Table 6). This is consistent with the findings of the research done by (Jacob et al., 2019, Kriedemann and Fester, 2015). In contrast, reduction of % yield value was observed when the temperature raised and similar finding was reported elsewhere that revealed the extract metabolites that were utilized to stabilize and cap the metal during the creation of nanoparticles are rendered inactive by the high temperature (Akintelu et al., 2021, Aksu Demirezen et al., 2022, Rajendran and Sen, 2016). As demonstrated in Table 6, room temperature resulted the best % yield value (27.40%) and used for the next optimization process.

Table 6: Effective diameters and yield values of IONPs synthesized utilizing banana peels extract at different temperature

Independent variables					**Dependent variables**	
$FeCl_3.6H_2O$ Conc. In M	**Ratio P. Ext.:Precu.**	**pH**	**T^0 (^0C)**	**Reaction Time In hr**	**Yield value (%)**	**Effective Diameter(nm)**
0.5	**1:2**	**12**	**Room**	**0.5**	**27.40**	**89.1**
0.5	1:2	12	40^0C	0.5	15.55	97.4
0.5	1:2	12	60^0C	0.5	11.85	113.1
0.5	1:2	12	80^0C	0.5	11.11	117.2
0.5	1:2	12	100^0C	0.5	8.15	120.5

5.2.2.5. Reaction time

Reaction time is a significant component that affects the shape of NPs along with temperature and pH (Karade et al., 2018). NPs produced from plant extract depend on the duration for which the reaction is incubated. The variation of the product with the duration of the reaction time may be due to the aggregation of particles (Kuchibhatla et al., 2012). The percentage yield value and particle size of the formed IONPs showed almost a vise versa trend with increased reaction time (Table 7), as the % yield value decreased the particle size increased. This might be as a result of long reaction time that cause aggregation and shrinkage of NPs (Akintelu et al., 2021). Other researchers have found that the particle dimensions were increased in extending the reaction time (Karade et al., 2018, Rose et al., 2016). The reaction time of 1hour gave best yield value (35.55%) and particle size (67.3nm). This result was equivalent to a study by Hong and Jiang (2017) that compared the percentage yield of synthetic SnO2 with reaction time, and revealed that the maximum percentage yield was achieved around 40 minutes (Hong and Jiang, 2017).

Table 7: Effective diameters and yield values of IONPs synthesized utilizing banana peels extract at different reaction time.

Independent variables					**Dependent variables**	
$FeCl_3.6H_2O$ Conc. In M	**Ratio P. Ext.:Precu.**	**pH**	**T^0 (^0C)**	**Reaction Time In hr**	**Yield value (%)**	**Effective Diameter(nm)**
0.5	1:2	12	Room	0.5	27.40	89.1
0.5	**1:2**	**12**	**Room**	**1**	**35.55**	**67.3**
0.5	1:2	12	Room	2	24.81	103.7
0.5	1:2	12	Room	3	24.44	108.3
0.5	1:2	12	Room	4	18.11	110.9

So, the precursor concentration of 0.5M, the extract to precursor ratio of 1:2, the pH of 12, reaction time of 1hour and room temperature were the parameters selected in order to synthesize optimal IONPs using banana peels extract.

5.3. Drug loading to IONPs

5.3.1. Optimization of parameters for CIP-IONPs

Reaction time and drug concentration were the two-variable optimized during drug loading after determining the λ_{max} and drawing the calibration curves of CIP using ultraviolet and visible absorption spectrophotometer (ThermoFisher, Evolution 201, USA). The CIP λ_{max} (271) was obtained by running 2 µg/ml, 3 µg/ml, 4 µg/ml, 5 µg/ml, and 6 µg/ml of CIP standard solution. A straight line with R^2 of 0.9993 (appendix I) was acquired from the calibration curves for determination of CIP concentration in the supernatant solution of each optimization trials.

Through hydrophobic interactions and π–π stacking, IONPs have been once believed to load a variety of medicines with excellent loading capacities and encapsulation efficiency (Liu et al., 2020b). The detrimental effects associated with using too much of the carrier materials could be limited by high drug encapsulation effectiveness in nanostructures, which can help lower the cost of manufacturing and scaling up (Yu et al., 2018).

5.3.1.1. Reaction time

Reaction time is among the commonest factors that affect capacity for drug loading and effective encapsulation. In this study the capacity for drug loading and effective encapsulation in respect to mixing time were done at 7.5mM concentration of CIP. The findings of the current investigation showed that when the mixing time increased starting from 0.5 hours loading capacity and encapsulation efficiency increased up to some instance after that increased mixing time decreased the loading capability and efficiency of encapsulation (Figure 2). The mixing time at 1 hour gave relatively good result with 21.3% $\pm$ 0.26 and 39.3% $\pm$ 0.6, capacity for loading and efficiency of encapsulation, respectively (Figure 2). This might be due to prolonged mixing time dislodge the adsorbed drug from the NPs' surface. So, reaction time of 1 hour was selected for the next investigation of optimal loading and encapsulation effectiveness of IONPs at different CIP concentrations.

.

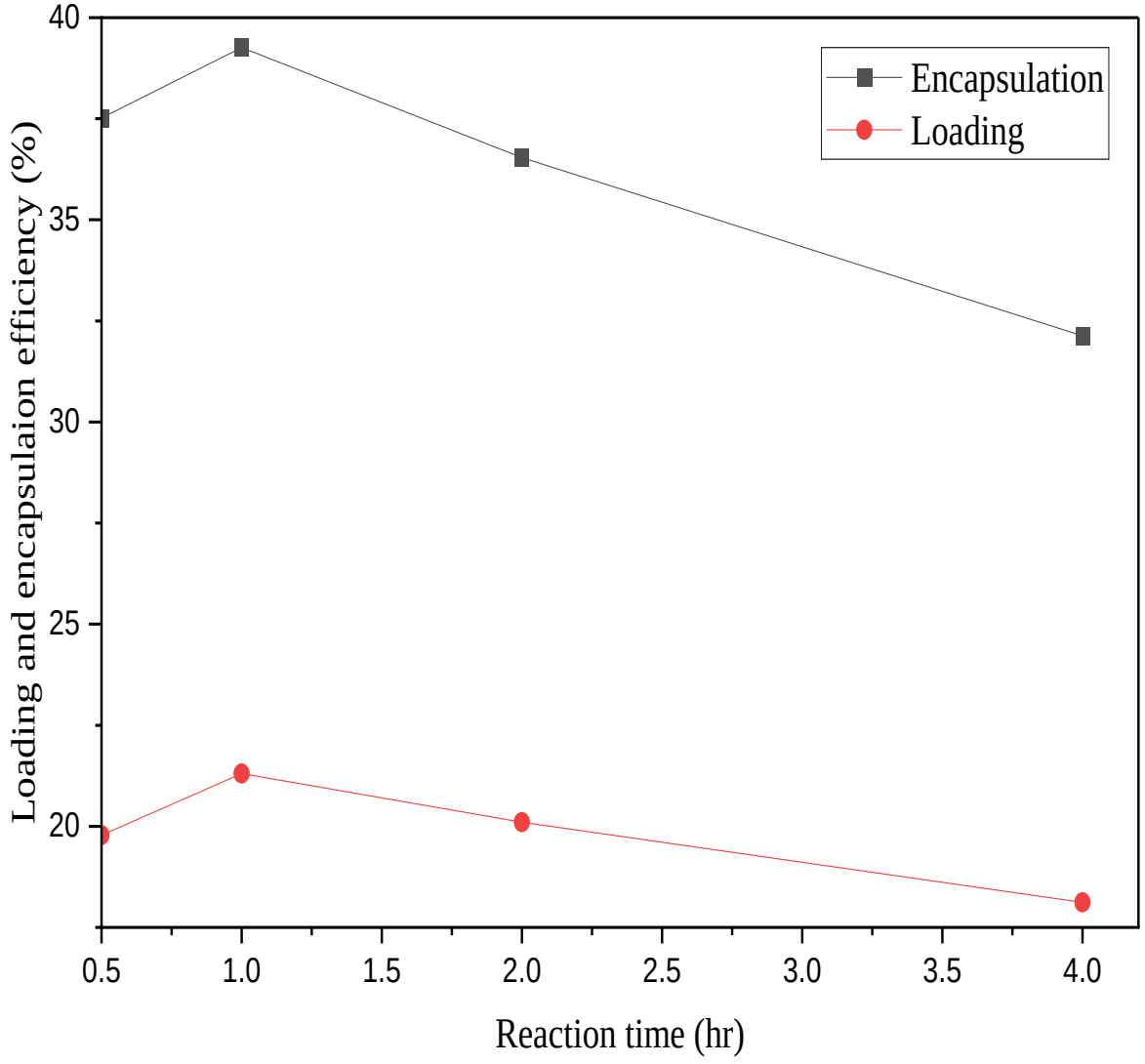

Figure 3: Loading and encapsulation effectiveness of IONPs with relation to time.

5.3.1.2. Drug concentration

Drug loading amount and encapsulation ability of NPs is believed to be one of the critical physicochemical characteristics assessed while developing various types of NPs. Drug concentration is one among the most popular factors in influencing the capacity of loading and encapsulation competence of NPs. The current study looked at the impact of the concentration of CIP on the capacity of loading and encapsulation competence was evaluated at optimal value of mixing time (1 hour) and the result found revealed that the stacking capacity and effectiveness of encapsulation of IONPs were increase when increased the concentration of CIP starting from

1.5mM to 10mM, but farther increased the concentration decreased the capacity of loading and encapsulation competence of IONPs (figure 3). Thus, CIP concentration of 10mM was found as a best optimized concentration for drug loading and encapsulation competence with 33.3% + 0.67 and 54% + 0.86. Liu et al, reported that the maximum loadings capacity of IONPs were ranged from 11.8–35.0 % due to their possession of large pores and large surface area (Liu et al., 2020b). Another study discovered that the void or mesoporous nature of IONPs allows for excessive drug loading capacity and rate of medicine release, both of which are critical needs for therapy (Lin et al., 2015).

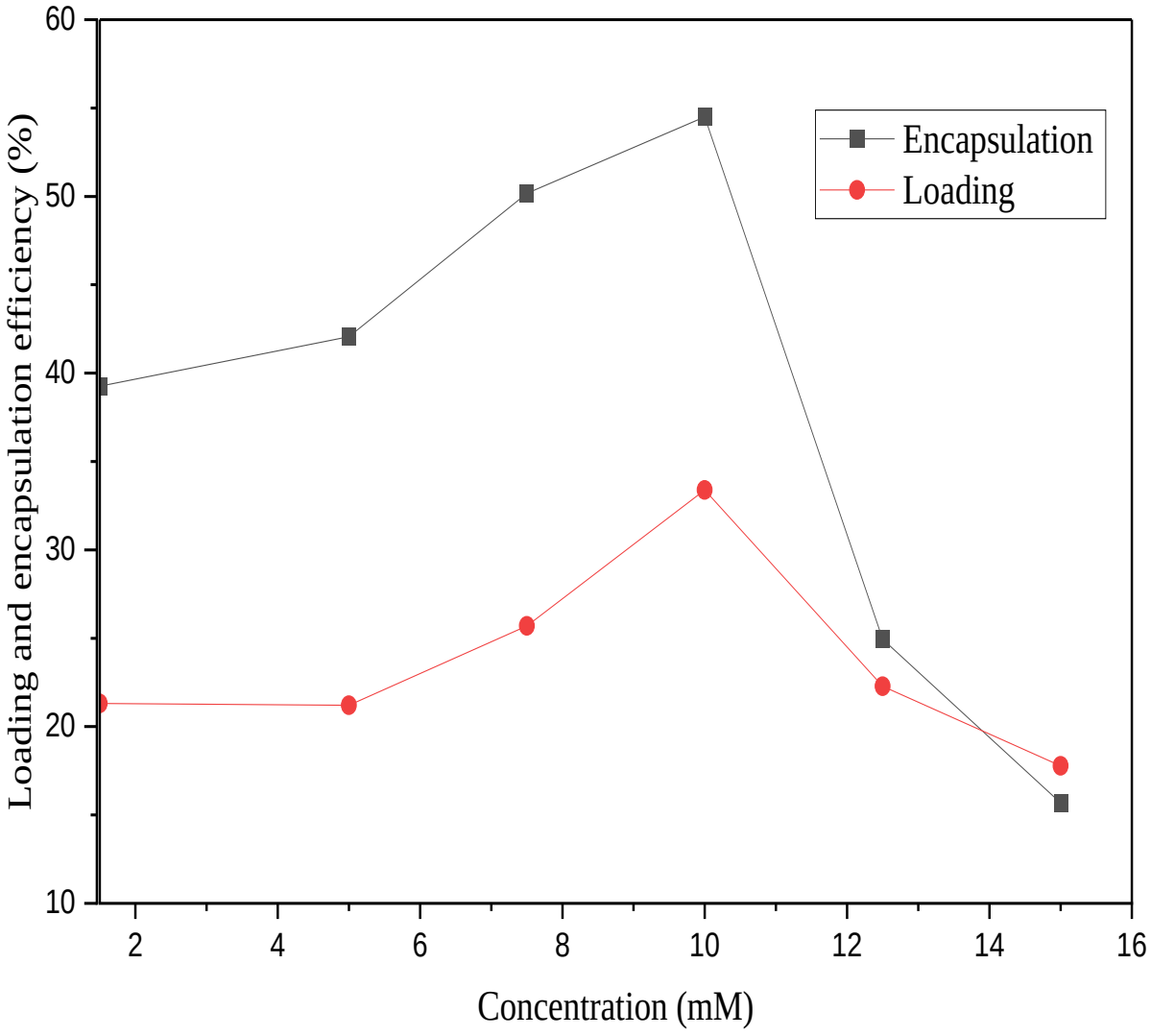

Figure 4: Loading and encapsulation efficiency of IONPs at a function of concentration.

5.4. Characterization of IONPs and CIP-IONPs

5.4.1. Dynamic light scattering (DLS) analysis

IONPs synthesized at optimal conditions had particles size of 67.3 nm ± 0.9 and polydispersity index (PDI) 0.242 ± 0.049 as shown in figure 4. This result is in agreement with the tolerable PDI which is less than 0.4 (Babick, 2020). This suggests that even if DLS overestimated the size, it may have been as a consequence of NPs' capacity to hold onto a certain quantity of water in aqueous suspension (Hao et al., 2019), The particle is within the acceptable range for the fabrication of NPs (Devi et al., 2019). The CIP-IONPs also showed with a particle dimensions 94 nm ± 2.1 and PDI of 0.254 ± 0.129. This may be owing to influence of medication loaded on its particle dimension because it is greater than the size of IONPs (Figure 5).

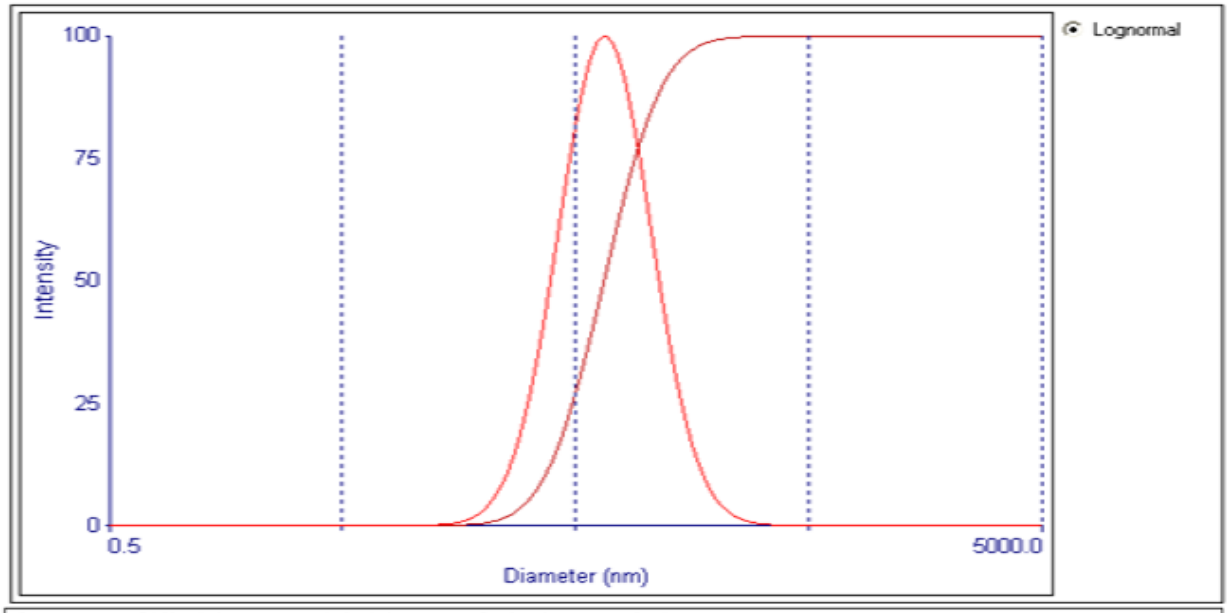

Run	Eff. Diam. (nm)	Half Width (nm)	Polydispersity	Baseline Index
1	67.7	27.4	0.164	0.0/ 18.41%
2	68.6	32.9	0.231	0.0/ 19.77%
3	65.5	37.7	0.331	6.4/ 10.33%
Mean	67.3	32.7	0.242	2.1/ 16.17%
Std. Error	0.9	3.0	0.049	2.1/ 2.94
Combined	67.0	32.1	0.230	0.0/ 16.17%

Figure 5: DLS graph of IONPs produced using banana peel extract.

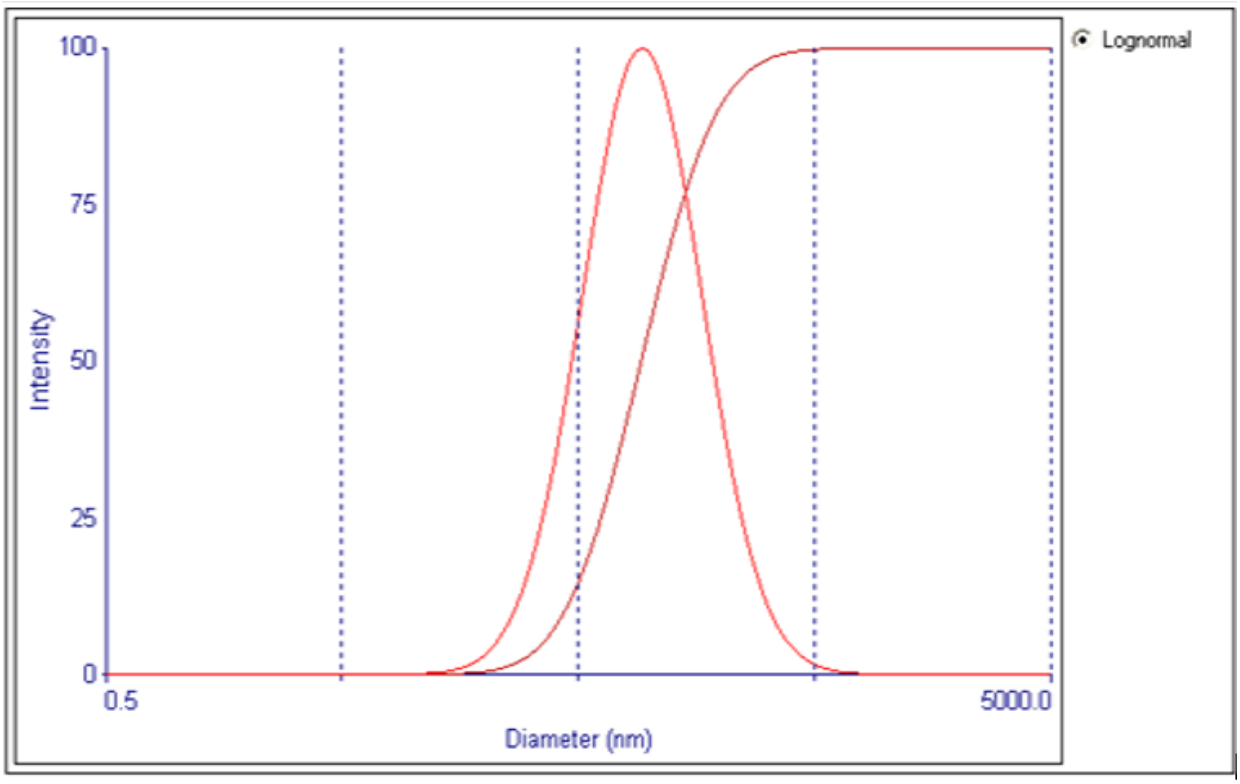

Run	Eff. Diam. (nm)	Half Width (nm)	Polydispersity	Baseline Index
1	97.3	64.4	0.437	0.0/ 8.02%
2	90.3	6.4	0.005	0.0/ 1.14%
3	94.4	53.2	0.318	0.0/ 4.01%
Mean	94.0	41.3	0.254	0.0/ 4.39%
Std. Error	2.1	17.8	0.129	0.0/ 1.99
Combined	93.5	59.3	0.403	0.0/ 4.39%

Figure 6: DLS graph of the CIP- IONPs.

5.4.2. UV visible spectrophotometer

For the appropriate conformation in terms of synthesis and loading of the drug, the UV visible spectrophotometric characterization of IONPs generated, CIP-IONPs, and CIP was performed. It was discovered that the unique UV absorption band at 272 nm (Figure 6) may be caused by the surface plasmon resonance effect of the IONPs produced, this corresponds to the literature (Ali et al., 2017, Sharma et al., 2020a). According to figure 7, the CIP-IONPs had a high peak at 352 nm and pure ciprofloxacin at 271 and 322 nm. This shows that there is some red shift when a

medication is loaded onto the NPs, which might be caused by a reduction in polarity of the loaded NPs.

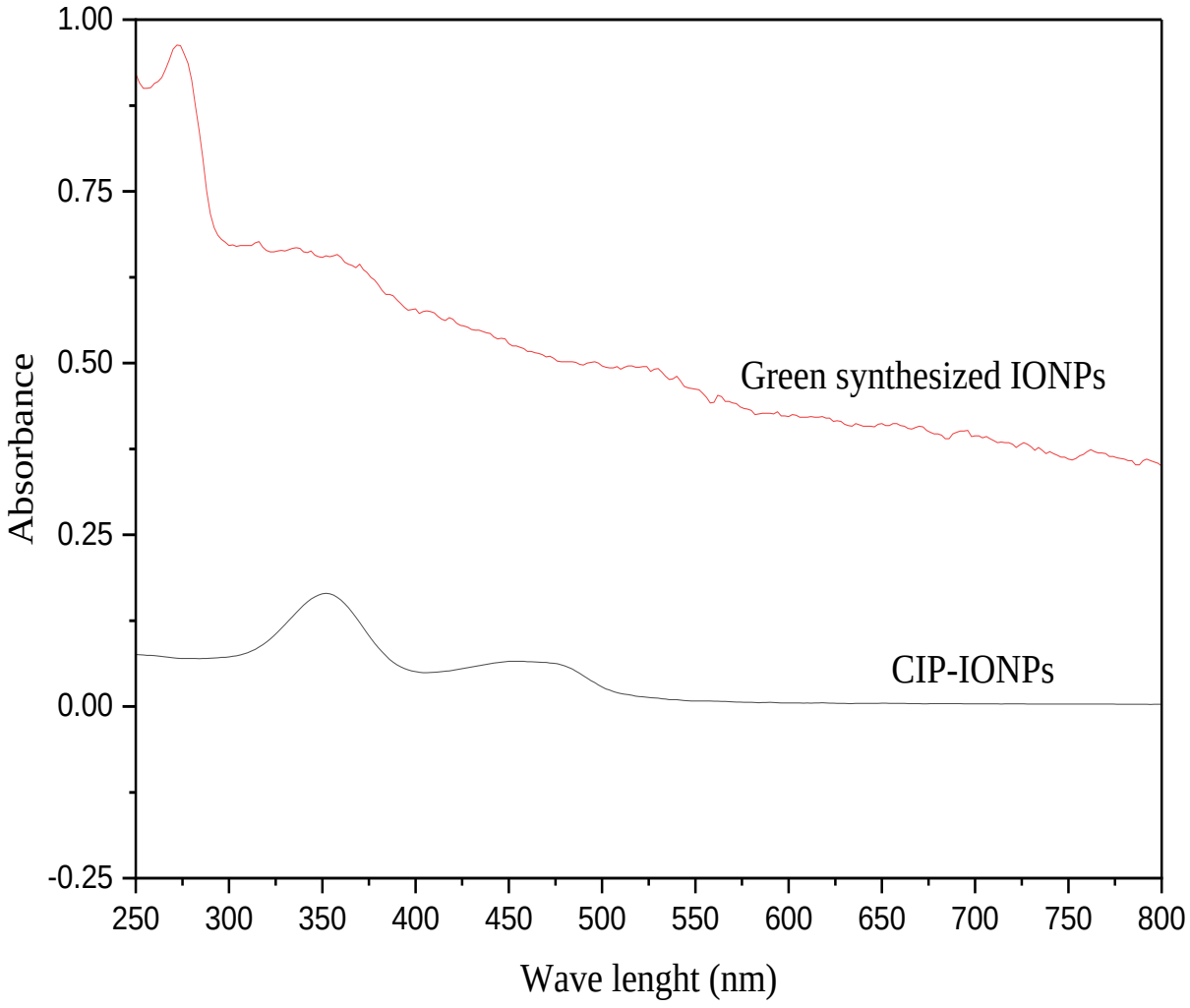

Figure 7: UV visible spectrums of green synthesized IONPs and CIP-IONPs.

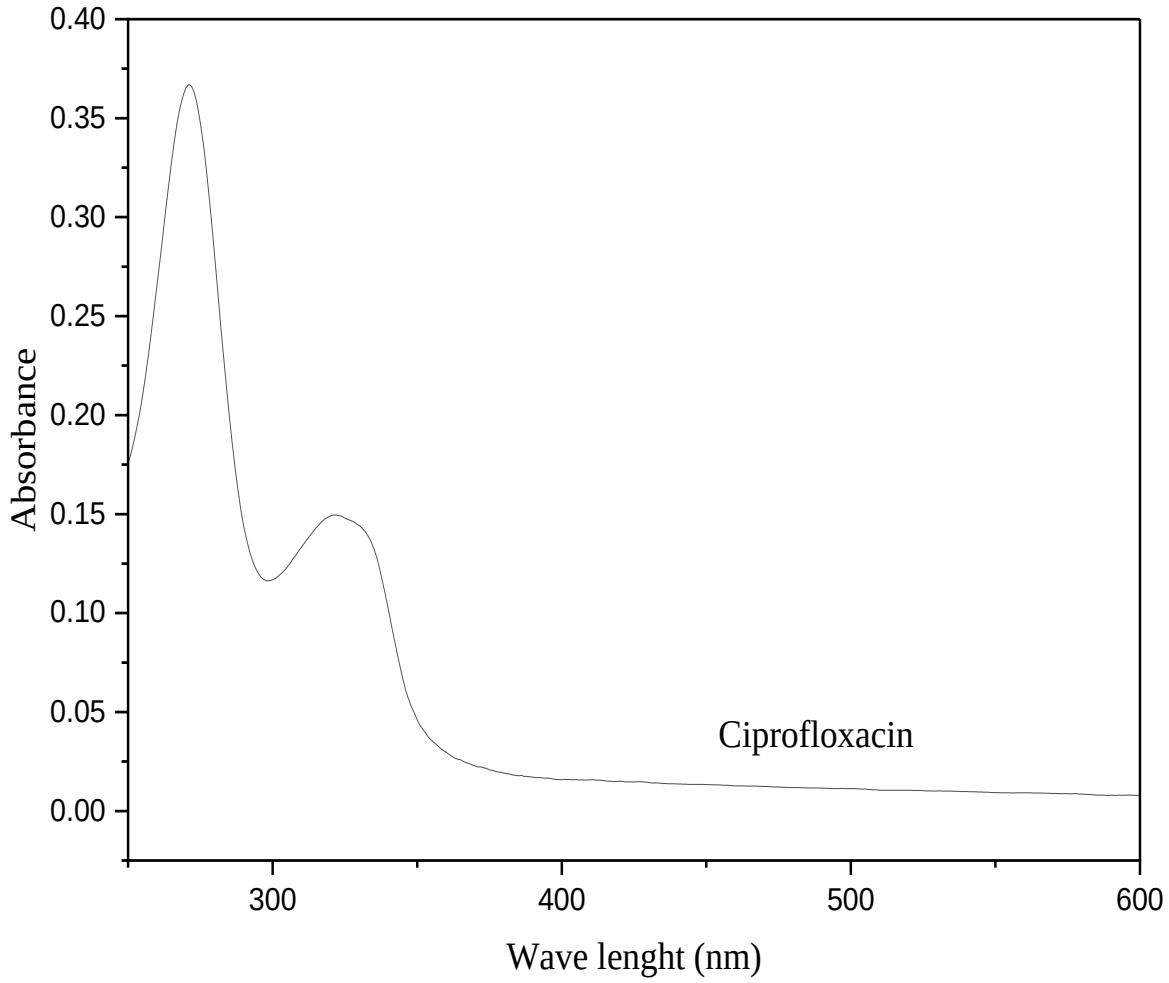

Figure 8: UV visible spectrums of pure CIP.

5.4.3. Fourier transform-infrared spectroscopic (FTIR) analysis

Figures 8, A and B, and Figure 9, A and B, respectively, show the described FTIR peaks of the extract of banana peels, IONPs, CIP-IONPs, and CIP.

The stretching of Fe-O functional groups, which is depicted by strong peaks at 461 cm-$^{-1}$ and 542 cm^{-1} in the IONPs peaks, clearly indicates the fabrication of hematite NPs. A peak on 1131 cm^{-1} is also present, and this peak serves as the hematite NPs' hallmark (Sharma et al., 2020b). On banana peel extract, IONPs, and CIP-IONPs, a distinctive peak at 3445 cm^{-1} is most likely originated by the existence of O-H functional groups, which may have come from the plant extract or, in the instance of IONP and CIP-IONPs, from adsorbed moisture and water molecule

during loading, respectively. The bulk of peaks seen in the extract of banana peels did not show up in the IONPs FTIR peaks (Figure 8). This might be because the organic plant extract components were degraded during the calcination of the NPs at 700^0c for two hours.

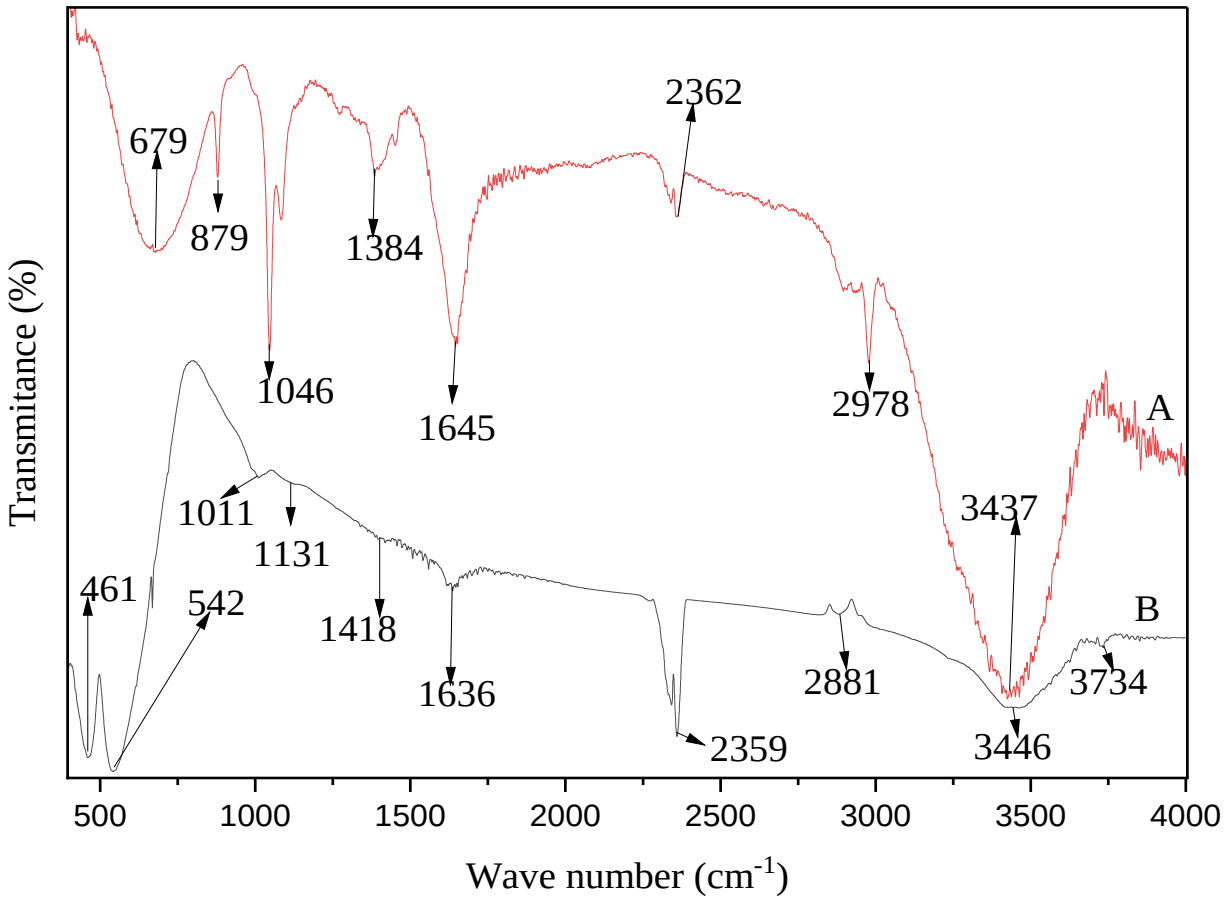

Figure 9: FTIR spectrums of (A) banana peels extract, and (B) IONPs

The relatively small amount of CIP in loaded NPs (33.3%), and moreover the moderate interaction of CIP and IONPs, maybe to account for the disappearance of some peaks and reduction in peak strength in the CIP-IONPs FTIR spectrum (Figure 9) (Ellerbrock and Gerke, 2021). The main functional group in the entire FTIR spectrum and its proposed indications are present in table 8.

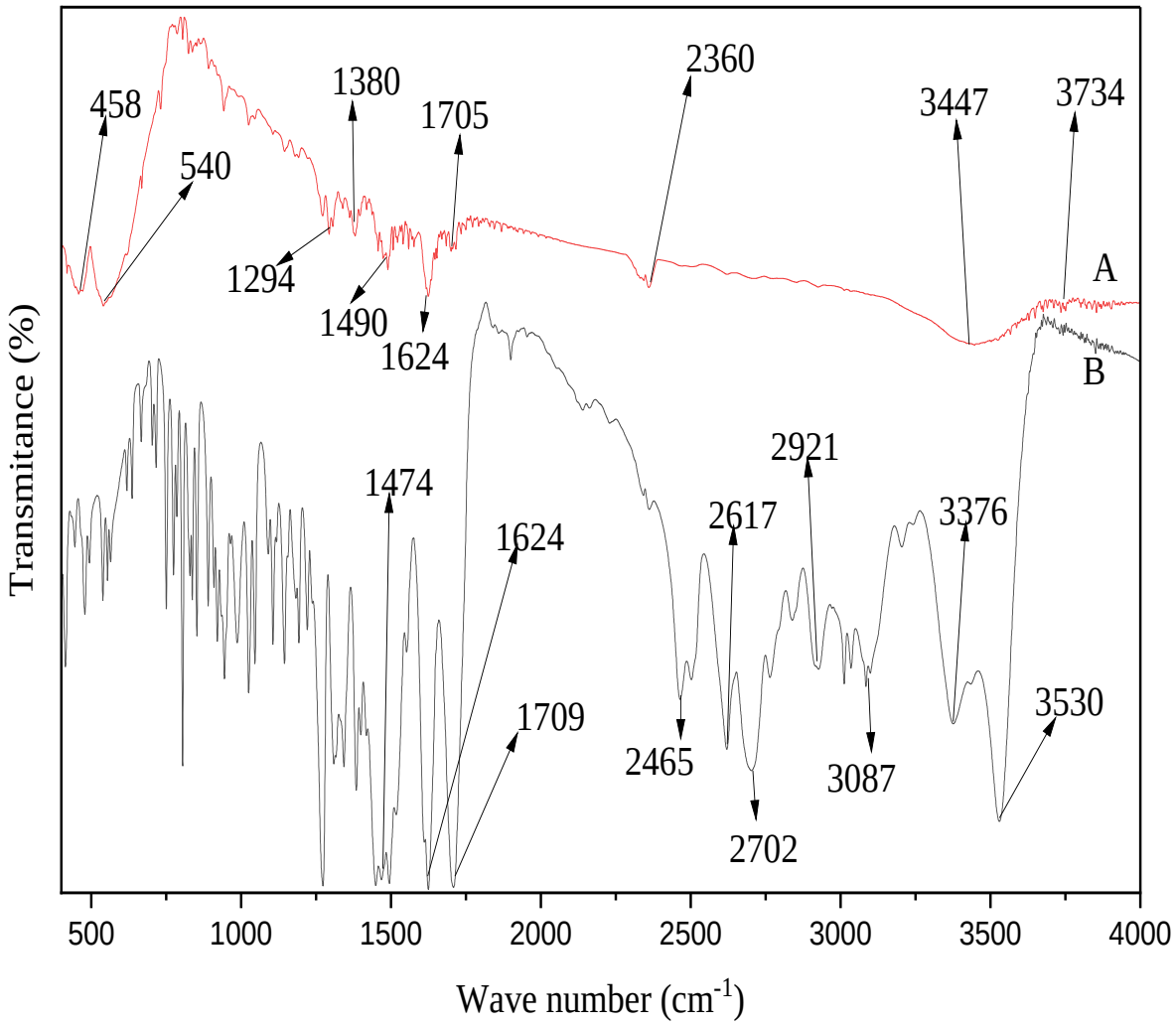

Figure 10: FTIR spectrums of (A) CIP-IONPOs, (B) CIP

Table 8: The main FTIR peaks of banana peel extract, IONPs CIP-IONPs and ciprofloxacin and their possible functional groups.

Wave numbers (Cm^{-1})	**Assigned stretching, bending, vibration or wag**	**Possible functional groups**	**Reference**
3445	O–H stretching	polyphenols or carboxylic acid	(Yi et al., 2019)
3537	stretching of C≡C alkyne or C-H stretching	aliphatic and aromatic compound	(Demirezen et al., 2019)
2932	Asymmetric and symmetric stretching of -CH2 and -CH3 functional groups	Aliphatic	(Ramesh et al., 2021)
2359	C=N C≡N or C-H stretching	aliphatic and aromatic compound	(Ramesh et al., 2021, Vinayagam et al., 2020)
1644	Amid I C–O vibration C = C bond	Protein/enzymes	(Sharma et al., 2020b)
1131	crystalline Fe–O vibrations	signature band for α-Fe_2O_3 NPs	(Sharma et al., 2020b, Vinayagam et al., 2020)
1012	C-O-C stretching C-N stretch N-H wag =C-H bend	Aromatics Aliphatic amines primary, secondary amine alkenes	(Eslami et al., 2018, Yan and Zhang, 2011)
542	Fe-O stretching vibrations	Hematite phase IONPs	(Bashir et al., 2019, Madubuonu

			et al., 2019)
461	Fe-O stretching vibrations	Hematite's NPs	(Bashir et al., 2019, Devi et al., 2019, Sharma et al., 2020b)

5.4.4. Powder x-ray diffraction (XRD) analysis

According to the XDR graph figure 10, at 2θ diffraction peaks values, 24.24^0, 33.28^0, 35.34^0, 40.93^0, 49.61^0, 54.19^0, and 62.23^0, with corresponding crystal planes (h, l, k) values of 012, 104, 110, 113, 024, 116, and 214, are a characteristic peak for hematite NPs, it is in agreement with other literature (Devi et al., 2019). The average calculated crystalline size from all peaks value (Table 9) using Debye Scherrer equation (Equation 3) gave 10.4 nm $\pm$ 1.98 which is in line with the DLS finding (67 nm) that is due to overestimating of DLS analysis (Devi et al., 2019).

Table 9: The mean size of synthesized IONPs calculated from XRD data using Debye Scherrer equation.

2θ (degree)	FWHM (degree)	Diameter (nm)	(h k l)
24.24	0.67421	12.05	012
33.28	0.86285	9.61	104
35.34	1.06721	7.81	110
40.93	0.64875	13.07	113
49.61	0.75597	11.58	024
54.19	0.85074	10.49	116
62.23	1.1363	8.17	214

FWHM: Full Width Half Maximum

The absence of any random peaks and sharp diffraction peaks in the XRD spectrum of the IONPs generated, respectively, served as indicators of the purity and crystallinity of the substance (Ahmmad et al., 2013). Peaks were consistent with the (File No. 01-076-4579 of the Joint Committee on Powder Diffraction Standards) as shown in figure 11.

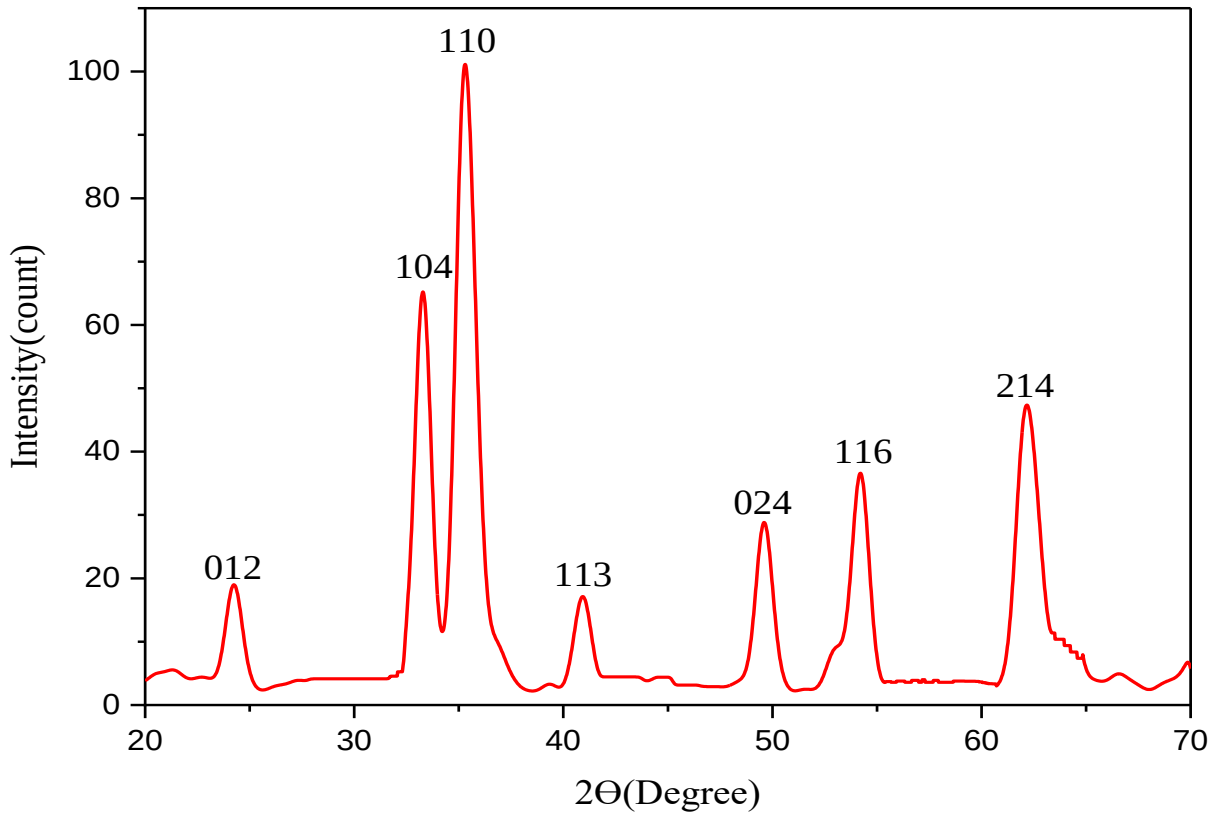

Figure 11: XRD pattern for IONPs synthesized utilizing bananas. peels extract.

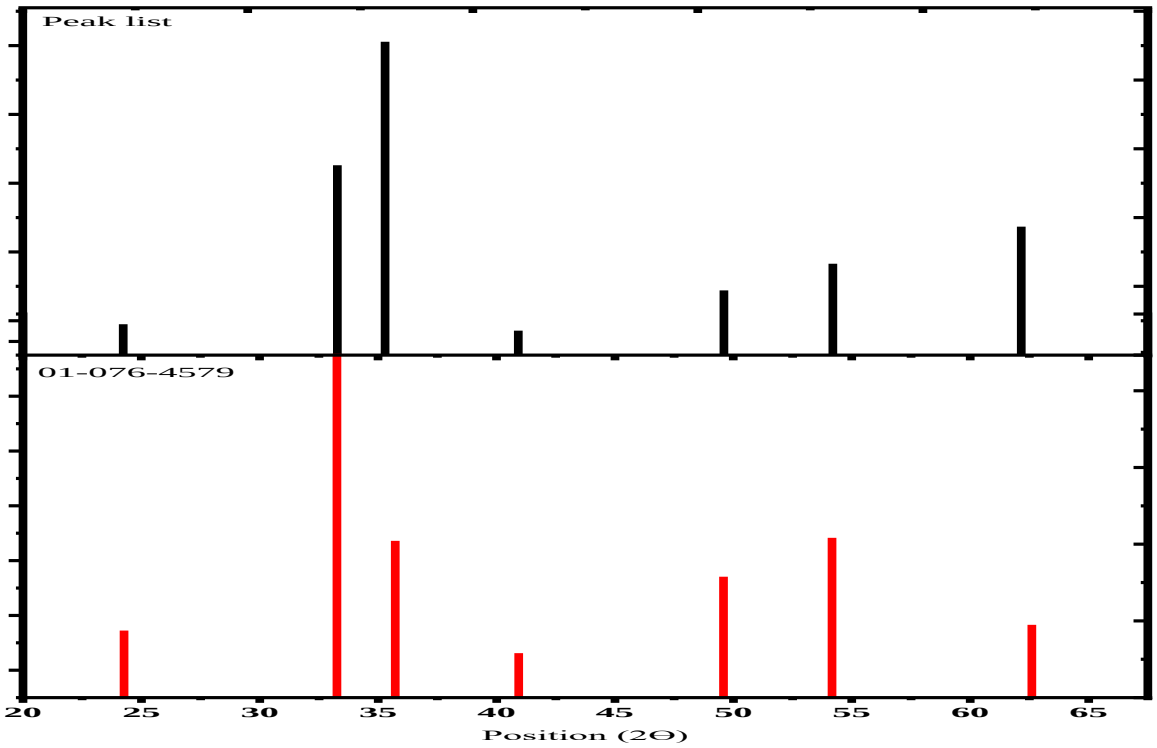

Figure 12: XRD pattern for green synthesized IONPs using banana peels extract with standard card comparison.

5.4.5. Scanning electron microscope (SEM) analysis

SEM pictures show the appearance, shape, and size of the NPs. For the current study, irregular and almost rod-shaped NPs were found (Figure 12A). Rod-shaped IONPs made using green synthesis techniques were also reported in several investigations (Anchan et al., 2019, Rather and Sundarapandian, 2020). The NPs' characteristically porous and powdery appearance showed that they had an inconsistent surface (Maji et al., 2012). According to some reports, the magnetic interactions of the NPs may lead to the creation of agglomerations that are evident in the SEM image (Anchan et al., 2019, de Jesús Ruíz-Baltazar et al., 2019, Natrayan et al., 2023). The mean calculated particle size ($48\ \text{nm} \pm 0.9$) of the IONPs using ImageJ software was relatively greater than the XRD crystalline size and smaller than DLS size of IONPs and this maybe as a result of agglomerations of the NPs and over estimation of the DLS technics respectively (Devi et al., 2019).

The surface roughness shown in figure 12B had good adsorbing capacity for drug loading (33.3%) which is almost the maximum loading capacity of IONPs reported in literature (11.5-35%) (Liu et al., 2020b) because it has been shown by researchers to have a faster antibacterial effect than a smooth surface (Sumedha and Andrea, 2016, Wang et al., 2019).

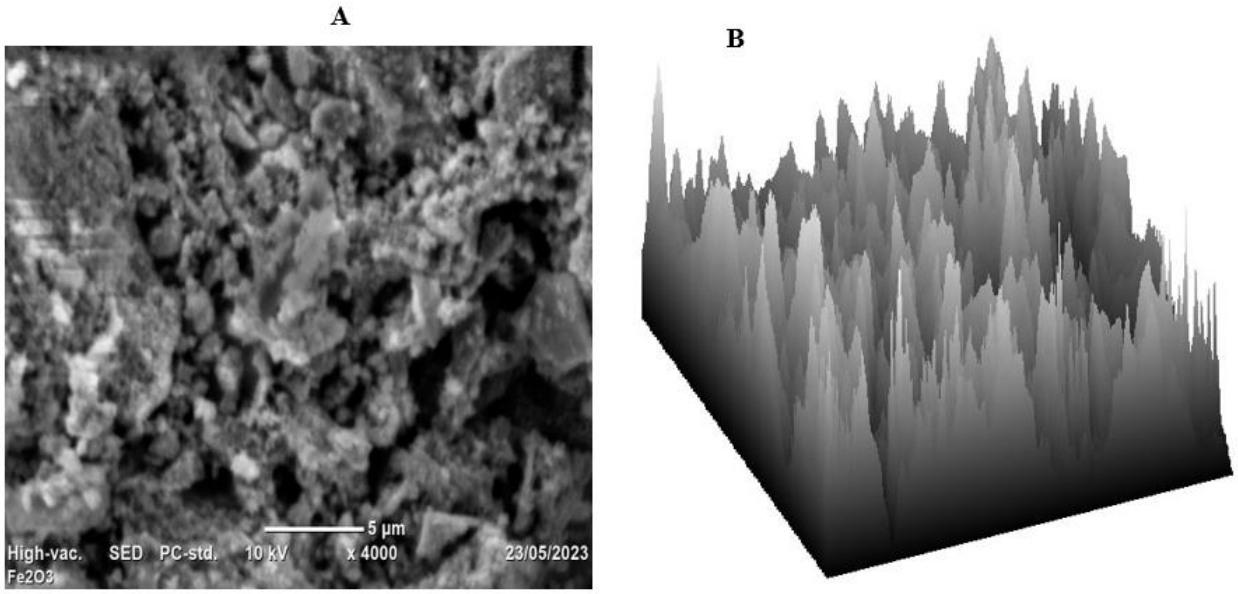

Figure 13: Image showing SEM of IONPs made from banana peel extract (A) particle shape, size and morphology, and (B) surface roughness.

5.4.6. Thermal analysis

The thermal examination of the IONPs created revealed no appreciable change in weight loss as temperature increased, demonstrating the remarkable heat stability of these NPs. The data showed two endothermic peaks, the first having a maximum limit of roughly 100°C and a decrease of mass of 0.34 percent of the total weight, and the second with a high at about 780°C and no mass loss in the DTG analysis (Figure 13). Dehydration of hygroscopic water is attributed to the first summit. The second peak is most likely as a result of a shift in crystal structure that occurs concurrently with a change to its crystalline state. Therefore, the small weight loss of roughly 100^0C caused by the water molecules evaporation that were attached to its surface of the NPs during processing time confirms the cleanliness of the NPs and is consistent with another investigation (Naz et al., 2019b).

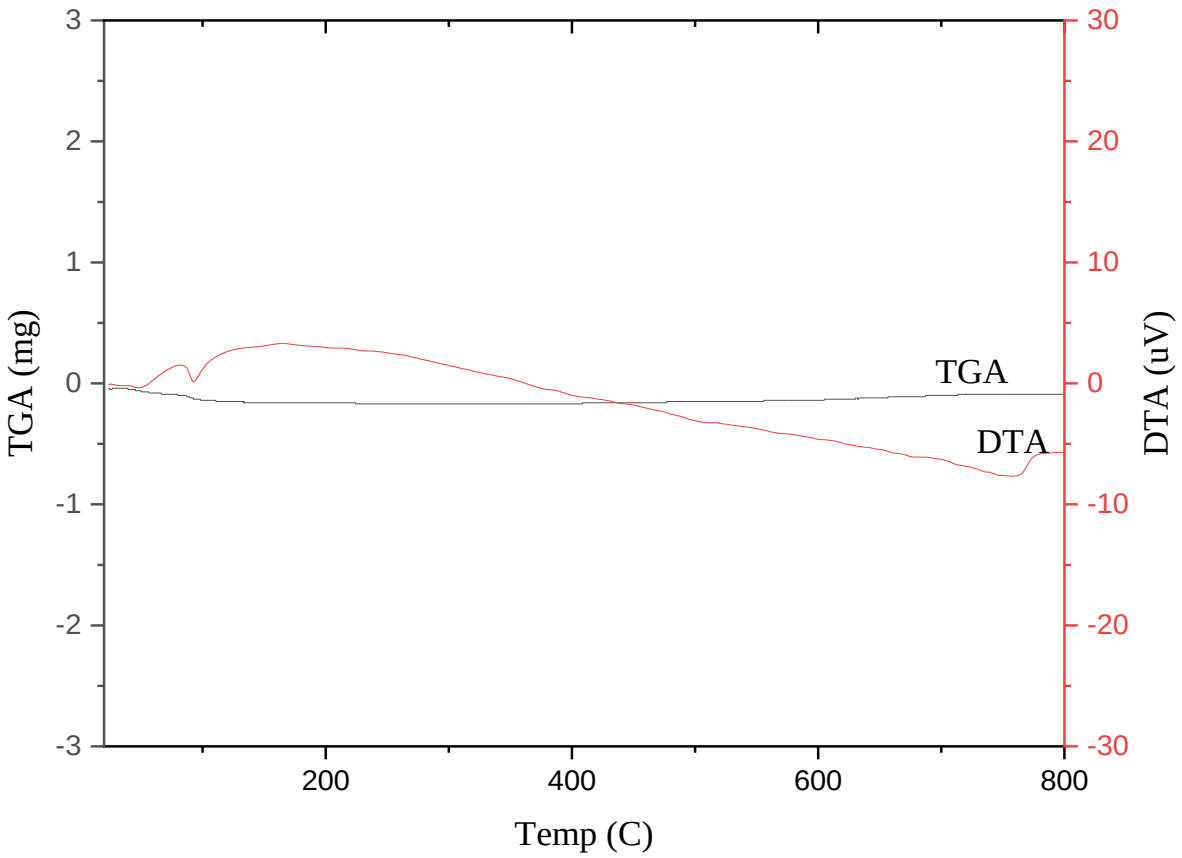

Figure 14: TGA Vs DTA analysis of IONPs synthesized using banana peels extract

5.5. *In vitro* drug release study

With correlation coefficients of 0.9995, 0.9994, and 0.9993 correspondingly (Table 10), the calibration curve of CIP employing stomach, intestine, and blood mimic fluids as a solvent produced a straight line (annex II).

Table 10: Calibration equation and correlation coefficients of CIP at different buffer solution

pH	λ_{max}	Linear questions	Correlation coefficients (R^2)
1.2	276nm	y = 105.2x + 0.0094	0.9995
6.8	271nm	y = 105.4x + 0.003	0.9994
7.4	270nm	y = 113x - 0.035	0.9993

This drug release investigation demonstrated that there are two patterns for CIP release that rely on the media's pH. The first was the rapid releasing pattern, which was 89.8% $\pm$ 0.1 (figure 14) within 4 hours in gastric fluid (pH 1.2). This pattern was also mentioned in other publications, and prior studies had also described a comparable CIP release from metallic NPs (Guo et al., 2018, Manatunga et al., 2017). It may be caused by burst releasing of the molecules of the drug that adsorb on the NP's outer most surface and as a consequence of relative acid solubility of CIP. In order to load CIP, Basu et al. produced semi-interpenetrating hydrogels of silver-nanocomposite that, after five hours, release 95% of the CIP (Basu et al., 2018). The release of 96.6% of CIP within 5 hours from gold nanocomposite hydrogel was also discovered in the study of (Prusty and Swain, 2019).

The second was a slow releasing pattern in intestinal and blood pH of 6.8 and 7.4 with 43.1% $\pm$ 0.6 and 29.6% $\pm$ 0.2 release rates within 4 hours respectively. This may be because CIP is less soluble in neutral media, this corresponds to research by Zafar et al. (2022) (Zafar et al., 2022). A study of Nawaz et al., revealed that CIP loaded gold nanoparticles had a similar releasing profile, with a 35% release rate within 4 hours (Nawaz et al., 2021a).

A pH-dependent U-shaped solubility of CIP with a minimum at pH 7.4 may account for why the releasing pattern of CIP at blood simulation fluids (pH 7.4) was slower than intestine simulation fluids, particularly from 2 hours to 16 hours (Figure 14) (Ross and Riley, 1990).

In general, the release profile of CIP in the current investigation exhibited two stages, which were roughly a raped release period up to around 5 hours and comparatively a delayed release after 5 hours in all simulation fluid (figure 14). The rapid release phase, in which the CIP-IONPs had a significant surface-to-volume proportion because of their small dimensions, which fosters fast release, served as confirmation of CIP adsorption on the outer layers of IONPs (Naz et al., 2013). As a consequence, the first burst release phase of 5 hours for CIP-IONPs may serve as a beginning dosage to prevent disease transmission, while the second, slower phase beyond 5 hours may assist offer a more effective therapeutic response, particularly in the blood and intestinal medium.

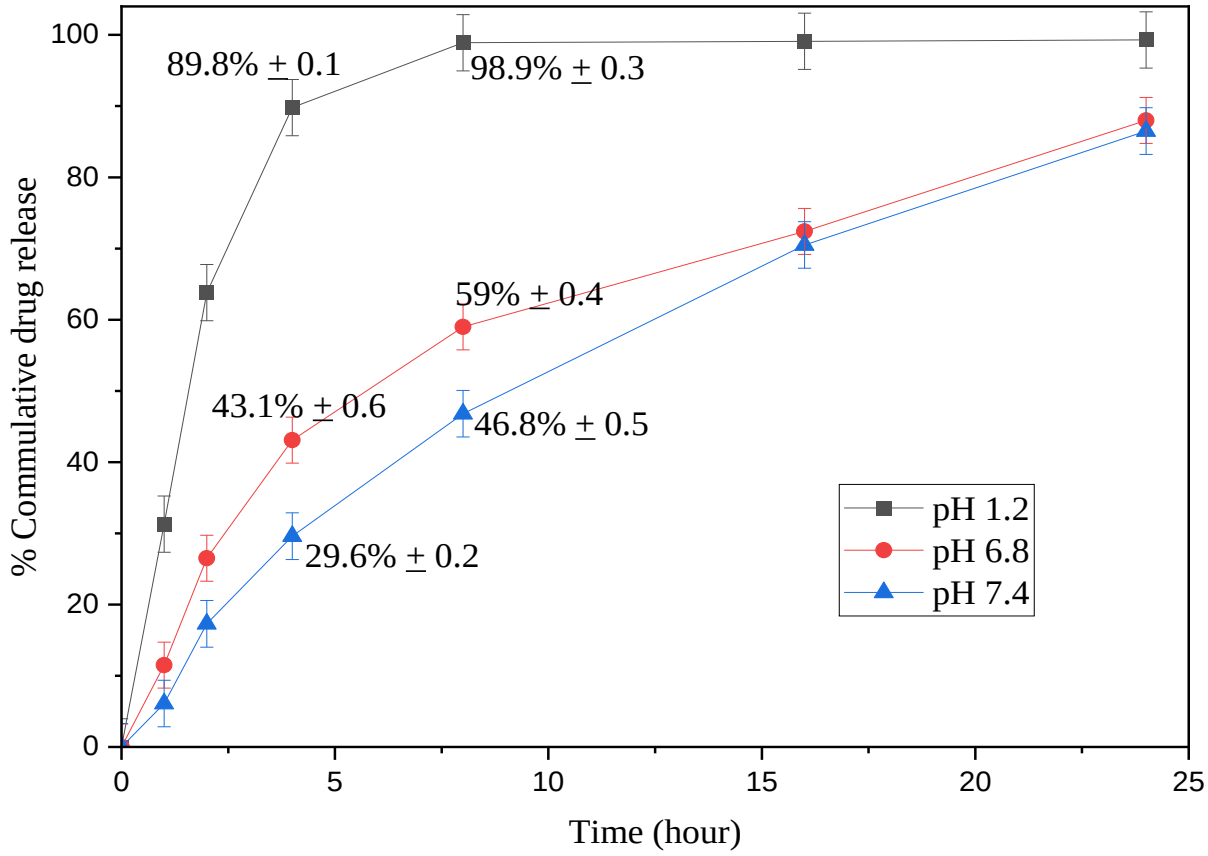

Figure 15: Percent cumulative drug release at different pH buffer solution of CIP-IONPs.

5.6. *In vitro* antimicrobial susceptibility study

The antibacterial susceptibility break point of a standard 5 µg of CIP for *E. coli* is classified as ≥26, 25-22, and ≤ 21, which, respectively, indicate sensitivity, intermediate susceptibility, and resistance (CLSI, 2021).

The potential antimicrobial mechanisms of IONPs for their antimicrobial activity include reactive oxygen species (ROS) generation, which has a genotoxic effect and damages DNA molecules (Kohanski et al., 2010, Zakariya et al., 2022), photocatalysis, Fenton reactions, vacuole formation, cell wall disruption, and inactivation of topoisomerase, which prevents DNA replication (Li et al., 2018). Additionally, the favorable charge on the exterior of metal NPs encourages their attachment with relation to the charged negative surface of the bacteria,

enhancing NPs' antibacterial action (Khezerlou et al., 2018). The NPs' bactericidal action is also influenced by their size (El Semary and Bakir, 2022, Menichetti et al., 2023, Mishra et al., 2022).

As result the of that in the current study antimicrobial susceptibility test using disc diffusion methods showed that IONPs have an antimicrobial bustle in opposition to CIP resistant *E. coli* with around 8mm ZOI (Table 11) which supported by different studies. According to a study IONPs had a ZOI of roughly 13 mm at strength of 1000 g/ml (1 g/l) (Yoonus et al., 2021) and this value is relatively higher than the current finding this might be due to higher concentration IONPs used relative to the current study (0.5µg/µl) and/or due to investigation of antimicrobial activity of IONPs against CIP resistant *E. coli* in the present research. Another study was discovered that hematite IONPs had antimicrobial action against *E. coli* with 9.5mm ZOI (Chihi et al., 2023) which is relatively comparable with result found in the this evaluation. The antimicrobial efficacy of IONPs for *E. coli* with 11mm ZOI was also demonstrated by (Saqib et al., 2019) which nearly comparable with this study finding. Baniasadi et al. likewise came to the realization that IONPs had a diverse variety of effects against bacteria that were highly resistant to antibiotics at very low concentrations (Baniasadi et al., 2020).

CIP-IONPs have a promising resistant reversal with a ZOI 22mm $\pm$ 0.15 which failed in intermediate susceptibility of antibacterial susceptibility break point indicated in CLSI 2021. But the ZOI (19 + 0.43) of CIP failed in the resistance category. Numerous investigations revealed that CIP's antibacterial effectiveness was improved when it was conjugated with various NPs, such as silver or gold (Kooti et al., 2018, Sreedharan and Singh, 2019). There are many metal and metal oxide nanoparticles (NPs) that include CIP that have more bacterial inhibitory activity than both CIP and the bare NPs (Maleki Dizaj et al., 2017, Mohsen et al., 2020, Nawaz et al., 2021b). The PCL-CIP-maghemite and PCL-CIP-hematite reduced bacterial growth with greater efficacy after 2 and 5 days of cultivation in the occurrence of a attracting field, according to research by (Sirivisoot and Harrison, 2015). Another study revealed that when CIP was contained in Graphene oxide-Cobalt ferrite-silver nanocomposite, its antiseptic action to *E. coli* ATCC® 25922TM was significantly increased (Kooti et al., 2018). Additionally, CIP's antibacterial activity was shown to have boosted when it was conjugated with gold nanoflowers by (Sreedharan and Singh, 2019).

The facilitation of IOPNs for conducting (passage) of CIP into bacterial (Rai et al., 2019), cell wall disruption effect of IONPs (Pelgrift and Friedman, 2013), protection of CIP from the resistance mechanisms of *E. coli* by IONPs (Huh and Kwon, 2011), interfere with the efflux pumping activity of *E.coli* (Banoee et al., 2010) and the ability of IONPs in reducing antibiotic resistance genes (ARGs) development in bacteria that are resistant to antibiotics (AlMatar et al., 2018) might be the possible mechanism for the effectiveness of CIP-IONPs over CIP alone.

The ability of Fe2O3 NPs to bind to the *E. coli* cell wall directly was demonstrated using the electron microscopy technique (Armijo et al., 2020). One of the antibacterial modes of action of NPs is to kill the bacterial cell by coming into close contact with the cell wall of the bacterial without penetrating in to the cell. As a result, NPs are less likely than antibiotics to cause bacterial resistance (Wang et al., 2017) and this might become one of the possible reasons of susceptibility of *E. coli* for CIP-IONPs.

In the current experiment, CIP's antibacterial activity with 19 + 0.43 mm ZOI (Table 11) showed that CIP was resistant to *E. coli*. This result was supported by a number of examinations and the currently popular global issue. In a study titled "Resistance Pattern of CIP Against Different Pathogens," that it was discovered about 27% of clinical isolates of *E. coli* were resistant to CIP (Ali et al., 2010). Neyestani et al., reported that a total of 28.03% of the 346 *E. coli* isolates obtained from different specimen in Iran were resistant to CIP (Neyestani et al., 2023). In a separate study, it came to light 122 (21.4%) out of a total of 569 clinical *E. coli* isolates from cases of community-acquired acute pyelonephritis were CIP-resistant (Kim et al., 2020).

Table 11: ZOI of IONP, CIP and CIP-IONP for *in vitro* antimicrobial study

Sample	**ZOI diameter (mm)[a]**	***In vitro* AST breaking point (CLSI, 2021)**
IONPs	8 ± 0.27	R
CIP	19 ± 0.43	R
CIP-IONPs	22 ± 0.15	I
Solvent (water)	6 ± 00	NA

AST: Antibacterial susceptibility test

I: Intermediate susceptibility

NA: Not applicable

R: Resistance

[a] Diameter measurement includes the disc diameter.

6. Conclusions

The series of optimized experimental methods utilized in this research enabled IONP production with 67.3 nm-sized nanometric particles. With a yield value of 35.55%, IONP synthesis utilizing banana peel extract under optimal processing conditions produced compounds with the required physicochemical characteristics. The obtained results showed that the synthesized IONPs had the best promising encapsulation efficiency and medication loading capability. CIP-IONPs had a fast drug releasing profile in gastric simulation fluid and relatively slow drug releasing profile in intestinal and blood simulation fluid. The antibacterial effectiveness of CIP against resistant *E. coli* was improved by IONPs.

As a result, the findings of this work suggest that biosynthesized IONPs made using extract from banana peels could be a suitable nano-carrier for CIP against *E. coli* resistance reversal.

7. Recommendations

The present study's findings suggested that additional research be done in the following areas.

- Short-term and long-term stability studies,
- Toxicity evaluation
- *In-vivo* drug release studies
- *In-vivo* antimicrobial susceptibility tests

8. References

ABOYEWA, J. A., SIBUYI, N. R., MEYER, M. & OGUNTIBEJU, O. O. 2021. Green synthesis of metallic nanoparticles using some selected medicinal plants from southern africa and their biological applications. *Plants,* 10**,** 1929.

AHMED, S. S., SHARIQ, A., ALSALLOOM, A. A., BABIKIR, I. H. & ALHOMOUD, B. N. 2019. Uropathogens and their antimicrobial resistance patterns: Relationship with urinary tract infections. *International journal of health sciences,* 13**,** 48-55.

AHMMAD, B., LEONARD, K., ISLAM, M. S., KURAWAKI, J., MURUGANANDHAM, M., OHKUBO, T. & KURODA, Y. 2013. Green synthesis of mesoporous hematite (α-Fe2O3) nanoparticles and their photocatalytic activity. *Advanced Powder Technology,* 24**,** 160-167.

AKINTELU, S. A., OYEBAMIJI, A. K., OLUGBEKO, S. C. & FOLORUNSO, A. S. 2021. Green synthesis of iron oxide nanoparticles for biomedical application and environmental remediation: a review. *Eclética Química,* 46**,** 17-37.

AKSU DEMIREZEN, D., YıLMAZ, Ş., DEMIREZEN YıLMAZ, D. & YıLDıZ, Y. Ş. 2022. Green synthesis of iron oxide nanoparticles using Ceratonia siliqua L. aqueous extract: improvement of colloidal stability by optimizing synthesis parameters, and evaluation of antibacterial activity against Gram-positive and Gram-negative bacteria. *International Journal of Materials Research,* 113**,** 849-861.

AL-HAKKANI, M. F., GOUDA, G. A. & HASSAN, S. H. A. 2021. A review of green methods for phyto-fabrication of hematite (α-Fe2O3) nanoparticles and their characterization, properties, and applications. *Heliyon,* 7.

AL-MQBALI, L. R. A. & HOSSAIN, M. A. 2019. Cytotoxic and antimicrobial potential of different varieties of ripe banana used traditionally to treat ulcers. *Toxicology Reports,* 6**,** 1086-1090.

ALBUQUERQUE, M. T. P., VALERA, M. C., MOREIRA, C. S., BRESCIANI, E., DE MELO, R. M. & BOTTINO, M. C. 2015. Effects of Ciprofloxacin-containing Scaffolds on Enterococcus faecalis Biofilms. *Journal of Endodontics,* 41**,** 710-714.

ALI, A., PAN, M., TILLY, T. B., ZIA, M. & WU, C. Y. 2018. Performance of silver, zinc, and iron nanoparticles-doped cotton filters against airborne E. coli to minimize bioaerosol exposure. *Air Quality, Atmosphere and Health,* 11**,** 1233-1242.

ALI, A., ZAFAR, H., ZIA, M., UL HAQ, I., PHULL, A. R., ALI, J. S. & HUSSAIN, A. 2016. Synthesis, characterization, applications, and challenges of iron oxide nanoparticles. *Nanotechnology, Science and Applications,* 9**,** 49-67.

ALI, H. R., NASSAR, H. N. & EL-GENDY, N. S. 2017. Green synthesis of α-Fe2O3 using Citrus reticulum peels extract and water decontamination from different organic pollutants. *Energy Sources, Part A: Recovery, Utilization, and Environmental Effects,* 39**,** 1425-1434.

ALI, S. Q., ZEHRA, A., NAQVI, B. S., SHAH, S. & BUSHRA, R. 2010. Resistance pattern of ciprofloxacin against different pathogens. *Oman medical journal,* 25**,** 294.

ALMATAR, M., MAKKY, E. A., VAR, I. & KOKSAL, F. 2018. The role of nanoparticles in the inhibition of multidrug-resistant bacteria and biofilms. *Current drug delivery,* 15**,** 470-484.

ALZATE, A. S., DÍAZ CARRILLO, Á. J., FLÓREZ-LÓPEZ, E. & GRANDE-TOVAR, C. D. 2021. Recovery of Banana Waste-Loss from Production and Processing: A Contribution to a Circular Economy. *Molecules (Basel, Switzerland),* 26**,** 1-30.

AMINI, K., AMIR, BIRCH, J. & BEKHIT, A. E.-D. A. 2019. Production, application and health effects of banana pulp and peel flour in the food industry. *Journal of food science and technology,* 56**,** 548-559.

ANAL, A. K., JAISANTI, S. & NOOMHORM, A. 2014. Enhanced yield of phenolic extracts from banana peels (Musa acuminata Colla AAA) and cinnamon barks (Cinnamomum varum) and their antioxidative potentials in fish oil. *Journal of Food Science and Technology,* 51**,** 2632-2639.

ANCHAN, S., PAI, S., SRIDEVI, H., VARADAVENKATESAN, T., VINAYAGAM, R. & SELVARAJ, R. 2019. Biogenic synthesis of ferric oxide nanoparticles using the leaf extract of Peltophorum pterocarpum and their catalytic dye degradation potential. *Biocatalysis and Agricultural Biotechnology,* 20**,** 101251.

ANDRADE, Â. L., SOUZA, D. M., PEREIRA, M. C., FABRIS, J. D. & DOMINGUES, R. Z. 2010. pH effect on the synthesis of magnetite nanoparticles by the chemical reduction-precipitation method. *Química Nova,* 33**,** 524-527.

ARAFA, M. G., MOUSA, H. A. & AFIFI, N. N. 2020. Preparation of PLGA-chitosan based nanocarriers for enhancing antibacterial effect of ciprofloxacin in root canal infection. *Drug Delivery,* 27**,** 26-39.

ARAGAW, T. A., BOGALE, F. M. & ARAGAW, B. A. 2021. Iron-based nanoparticles in wastewater treatment: A review on synthesis methods, applications, and removal mechanisms. *Journal of Saudi Chemical Society,* 25**,** 101280.

ARAKHA, M., PAL, S., SAMANTARRAI, D., PANIGRAHI, T. K., MALLICK, B. C., PRAMANIK, K., MALLICK, B. & JHA, S. 2015. Antimicrobial activity of iron oxide nanoparticle upon modulation of nanoparticle-bacteria interface. *Scientific Reports,* 5**,** 1-12.

ARAMI, H., KHANDHAR, A., LIGGITT, D. & KRISHNAN, K. M. 2015. In vivo delivery, pharmacokinetics, biodistribution and toxicity of iron oxide nanoparticles. *Chemical Society Reviews,* 44**,** 8576-8607.

ARCHANA, V., JOSEPH PRINCE, J. & KALAINATHAN, S. 2021. Simple one-step leaf extract-assisted preparation of α-Fe2O3 nanoparticles, physicochemical properties, and its sunlight-driven photocatalytic activity on methylene blue dye degradation. *Journal of Nanomaterials,* 2021**,** 1-25.

ARIAS, L. S., PESSAN, J. P., VIEIRA, A. P. M., LIMA, T. M. T. D., DELBEM, A. C. B. & MONTEIRO, D. R. 2018. Iron oxide nanoparticles for biomedical applications: A perspective on synthesis, drugs, antimicrobial activity, and toxicity. *Antibiotics,* 7**,** 46.

ARMIJO, L. M., WAWRZYNIEC, S. J., KOPCIUCH, M., BRANDT, Y. I., RIVERA, A. C., WITHERS, N. J., COOK, N. C., HUBER, D. L., MONSON, T. C. & SMYTH, H. D. 2020. Antibacterial activity of iron oxide, iron nitride, and tobramycin conjugated nanoparticles against Pseudomonas aeruginosa biofilms. *Journal of Nanobiotechnology,* 18**,** 1-27.

ARUNA, V., MUNDRU, K., AISHWARYA, C., MOKKAPATI, V. & DHULIPALLA, B. S. 2023. Metal-based nanosystems and the evaluation of their antimicrobial activity. *Antimicrobial Nanosystems.* Elsevier.

ASOUFI, H. M., AL-ANTARY, T. M. & AWWAD, A. M. 2018. Green route for synthesis hematite (α-Fe 2 O 3) nanoparticles: Toxicity effect on the green peach aphid, Myzus

persicae (Sulzer). *Environmental Nanotechnology, Monitoring & Management,* 9**,** 107-111.

ASSALI, M., ZAID, A. N., ABDALLAH, F., ALMASRI, M. & KHAYYAT, R. 2017. Single-walled carbon nanotubes-ciprofloxacin nanoantibiotic: Strategy to improve ciprofloxacin antibacterial activity. *International Journal of Nanomedicine,* 12**,** 6647-6659.

AZARGUN, R., BARHAGHI, M. H. S., KAFIL, H. S., OSKOUEE, M. A., SADEGHI, V., MEMAR, M. Y. & GHOTASLOU, R. 2019. Frequency of DNA gyrase and topoisomerase IV mutations and plasmid-mediated quinolone resistance genes among Escherichia coli and Klebsiella pneumoniae isolated from urinary tract infections in Azerbaijan, Iran. *Journal of Global Antimicrobial Resistance,* 17**,** 39-43.

BABICK, F. 2020. Dynamic light scattering (DLS). *Characterization of Nanoparticles.* Elsevier.

BAKHTIARY, Z., SAEI, A. A., HAJIPOUR, M. J., RAOUFI, M., VERMESH, O. & MAHMOUDI, M. 2016. Targeted superparamagnetic iron oxide nanoparticles for early detection of cancer: Possibilities and challenges. *Nanomedicine: Nanotechnology, Biology and Medicine,* 12**,** 287-307.

BALAMURUGAN, M., SARAVANAN, S. & SOGA, T. 2014. Synthesis of iron oxide nanoparticles by using eucalyptus globulus plant extract. *e-Journal of Surface Science and Nanotechnology,* 12**,** 363-367.

BANIASADI, N., KARIMINIK, A. & KHOSHROO, S. M. R. 2020. Synthesis and study of bactericidal effects of iron oxide nanoparticles on bacteria isolated from urinary tract infections. *Avicenna Journal of Clinical Medicine,* 27**,** 37-44.

BANOEE, M., SEIF, S., NAZARI, Z. E., JAFARI-FESHARAKI, P., SHAHVERDI, H. R., MOBALLEGH, A., MOGHADDAM, K. M. & SHAHVERDI, A. R. 2010. ZnO nanoparticles enhanced antibacterial activity of ciprofloxacin against Staphylococcus aureus and Escherichia coli. *Journal of Biomedical Materials Research Part B: Applied Biomaterials,* 93**,** 557-561.

BASHIR, A., FURQAN, C., BHARUTH-RAM, K., KAVIYARASU, K., TCHOKONTÉ, M. & MAAZA, M. 2019. Structural, optical and Mössbauer investigation on the biosynthesized α-Fe2O3: Study on different precursors. *Physica E: Low-dimensional Systems and Nanostructures,* 111**,** 152-157.

BASU, S., SAMANTA, H. S. & GANGULY, J. 2018. Green synthesis and swelling behavior of Ag-nanocomposite semi-IPN hydrogels and their drug delivery using Dolichos biflorus Linn. *Soft Materials,* 16**,** 7-19.

BAYDA, S., ADEEL, M., TUCCINARDI, T., CORDANI, M. & RIZZOLIO, F. 2020. The history of nanoscience and nanotechnology: From chemical-physical applications to nanomedicine. *Molecules,* 25**,** 1-15.

BELETE, M. A. & SARAVANAN, M. 2020. A systematic review on drug resistant urinary tract infection among pregnant women in developing countries in africa and asia; 2005-2016. *Infection and Drug Resistance,* 13**,** 1465-1477.

BIBI, I., NAZAR, N., ATA, S., SULTAN, M., ALI, A., ABBAS, A., JILANI, K., KAMAL, S., SARIM, F. M., KHAN, M. I., JALAL, F. & IQBAL, M. 2019. Green synthesis of iron oxide nanoparticles using pomegranate seeds extract and photocatalytic activity evaluation for the degradation of textile dye. *Journal of Materials Research and Technology,* 8**,** 6115-6124.

BISWAS, P., POLASH, S. A., DEY, D., KAIUM, M. A., MAHMUD, A. R., YASMIN, F., BARAL, S. K., ISLAM, M. A., RAHAMAN, T. I. & ABDULLAH, A. 2023. Advanced implications of nanotechnology in disease control and environmental perspectives. *Biomedicine & Pharmacotherapy,* 158**,** 114172.

BORIS, N. T. J., LAURETTE, N. N. & MODESTINE, K. S. M. 2023. Plantain (Musa paradisiaca L.): Production, Consumption and Processing in Cameroon. *American Journal of Food Science and Technology,* 11**,** 8-14.

CAAMANO, M. A. & CARRILLO, M. M. 2016. Iron Oxide Nanoparticle Improve the Antibacterial Activity of Erythromycin. *Journal of Bacteriology & Parasitology,* 07.

CHAKUPURAKAL, R., AHMED, M., SOBITHADEVI, D. N., CHINNAPPAN, S. & REYNOLDS, T. 2010. Urinary tract pathogens and resistance pattern. *Journal of Clinical Pathology,* 63**,** 652-654.

CHAMORRO, F., CARPENA, M., FRAGA-CORRAL, M., ECHAVE, J., RAJOKA, M. S. R., BARBA, F. J., CAO, H., XIAO, J., PRIETO, M. & SIMAL-GANDARA, J. 2022. Valorization of kiwi agricultural waste and industry by-products by recovering bioactive compounds and applications as food additives: A circular economy model. *Food Chemistry,* 370**,** 131315.

CHAUDHRY, F., AHMAD, M. L., HAYAT, Z., RANJHA, M. M. A. N., CHAUDHRY, K., ELBOUGHDIRI, N., ASMARI, M. & UDDIN, J. 2022. Extraction and Evaluation of the Antimicrobial Activity of Polyphenols from Banana Peels Employing Different Extraction Techniques. *Separations,* 9.

CHEN, L., XIE, J., WU, H., LI, J., WANG, Z., SONG, L., ZANG, F., MA, M., GU, N. & ZHANG, Y. 2018. Precise study on size-dependent properties of magnetic iron oxide nanoparticles for in vivo magnetic resonance imaging. *Journal of Nanomaterials,* 2018.

CHIHI, S., BOUAFIA, A., MENECEUR, S., LAOUINI, S. E. & AHMED, R. Z. 2023. Effect of precursor concentration on the bandgap energy and particles size for green synthesis of hematite α-Fe2O3 nanoparticles by the aqueous extract of Moltkia ciliata and evaluation of the antibacterial activity. *Biomass Conversion and Biorefinery***,** 1-14.

CHOMCHOEY, N., BHONGSUWAN, D. & BHONGSUWAN, T. 2018. Effect of calcination temperature on the magnetic characteristics of synthetic iron oxide magnetic nanoparticles for arsenic adsorption. *Chiang Mai J. Sci,* 45**,** 528.

DAGNEW, A., ASSEFA, W., KEBEDE, G. & AYELE, L. 2021. Evaluation of Banana (Musa spp .) Cultivars for Growth , Yield and Fruit Quality Bananas (Musa spp .) are important fruits in the tropics and subtropics . Ethiopia is. *Ethiopian Journal Agricuture,* 31**,** 1-25.

DE JESÚS RUÍZ-BALTAZAR, Á., REYES-LÓPEZ, S. Y., DE LOURDES MONDRAGÓN-SÁNCHEZ, M., ROBLES-CORTÉS, A. I. & PÉREZ, R. 2019. Eco-friendly synthesis of Fe3O4 nanoparticles: evaluation of their catalytic activity in methylene blue degradation by kinetic adsorption models. *Results in Physics,* 12**,** 989-995.

DEBEBE, A. D. & DAGNE, D. 2018. Analysis of socio-economic factors affecting banana production: Evidences from lowlands of uba debretsehay Woreda, Gamo Gofa Zone, SNNPRS. *Journal of Economics and Sustainable Development,* 9**,** 1-7.

DEHSARI, H. S., RIBEIRO, A. H., ERSÖZ, B., TREMEL, W., JAKOB, G. & ASADI, K. 2017. Effect of precursor concentration on size evolution of iron oxide nanoparticles. *CrystEngComm,* 19**,** 6694-6702.

DEMIREZEN, D. A., YıLDıZ, Y. Ş., YıLMAZ, Ş. & YıLMAZ, D. D. 2019. Green synthesis and characterization of iron oxide nanoparticles using Ficus carica (common fig) dried fruit extract. *Journal of bioscience and bioengineering,* 127**,** 241-245.

DEVI, H. S., BODA, M. A., SHAH, M. A., PARVEEN, S. & WANI, A. H. 2019. Green synthesis of iron oxide nanoparticles using Platanus orientalis leaf extract for antifungal activity. *Green Processing and Synthesis,* 8**,** 38-45.

DHARR, A., ARJUN, A., RAGURAM, T. & RAJNI, K. 2020. Influence of pH on the structural, spectral, optical, morphological and photocatalytic properties of ZrO2 nanoparticles synthesized by sol–gel technique. *Journal of Materials Science: Materials in Electronics,* 31**,** 15718-15730.

DOWLATH, M. J. H., MUSTHAFA, S. A., MOHAMED KHALITH, S. B., VARJANI, S., KARUPPANNAN, S. K., RAMANUJAM, G. M., ARUNACHALAM, A. M., ARUNACHALAM, K. D., CHANDRASEKARAN, M., CHANG, S. W., CHUNG, W. J. & RAVINDRAN, B. 2021. Comparison of characteristics and biocompatibility of green synthesized iron oxide nanoparticles with chemical synthesized nanoparticles. *Environmental Research,* 201**,** 111585-111585.

DREADEN, E. C., AUSTIN, L. A., MACKEY, M. A. & EL-SAYED, M. A. 2012. Size matters: Gold nanoparticles in targeted cancer drug delivery. *Therapeutic Delivery,* 3**,** 457-478.

EDGE, D., SHORTT, C. M., GOBBO, O. L., TEUGHELS, S., PRINA-MELLO, A., VOLKOV, Y., MACENEANEY, P., RADOMSKI, M. W. & MARKOS, F. 2016. Pharmacokinetics and bio-distribution of novel super paramagnetic iron oxide nanoparticles (SPIONs) in the anaesthetized pig. *Clinical and Experimental Pharmacology and Physiology,* 43**,** 319-326.

EDIS, Z., WANG, J., WAQAS, M. K., IJAZ, M. & IJAZ, M. 2021. Nanocarriers-mediated drug delivery systems for anticancer agents: an overview and perspectives. *International journal of nanomedicine***,** 1313-1330.

EL SEMARY, N. A. & BAKIR, E. M. 2022. Multidrug-resistant bacterial pathogens and public health: the antimicrobial effect of cyanobacterial-biosynthesized silver nanoparticles. *Antibiotics,* 11**,** 1003.

ELLERBROCK, R. H. & GERKE, H. H. 2021. FTIR spectral band shifts explained by OM–cation interactions. *Journal of Plant Nutrition and Soil Science,* 184**,** 388-397.

ERKAKAN, D., DIKER, N. Y., MÜŞERREF, Ö. & ÇANKAYA, İ. İ. 2022. Green synthesis of silver nanoparticles using Salvia fruticosa Mill. extract and the effect of synthesis

parameters on their formation, antioxidant, and electro-catalytic activity. *Hacettepe Journal of Biology and Chemistry,* 50**,** 397-414.

ESLAMI, S., EBRAHIMZADEH, M. A. & BIPARVA, P. 2018. Green synthesis of safe zero valent iron nanoparticles by Myrtus communis leaf extract as an effective agent for reducing excessive iron in iron-overloaded mice, a thalassemia model. *RSC advances,* 8**,** 26144-26155.

FASUGBA, O., GARDNER, A., MITCHELL, B. G. & MNATZAGANIAN, G. 2015. Ciprofloxacin resistance in community- and hospital-acquired Escherichia coli urinary tract infections: A systematic review and meta-analysis of observational studies. *BMC Infectious Diseases,* 15.

FATIMA, F., SIDDIQUI, S. & KHAN, W. A. 2021. Nanoparticles as novel emerging therapeutic antibacterial agents in the antibiotics resistant era. *Biological Trace Element Research,* 199**,** 2552-2564.

FENG, Q., LIU, Y., HUANG, J., CHEN, K., HUANG, J. & XIAO, K. 2018. Uptake, distribution, clearance, and toxicity of iron oxide nanoparticles with different sizes and coatings. *Scientific Reports,* 8**,** 1-13.

FLEITAS-SALAZAR, N., SILVA-CAMPA, E., PEDROSO-SANTANA, S., TANORI, J., PEDROZA-MONTERO, M. R. & RIERA, R. 2017. Effect of temperature on the synthesis of silver nanoparticles with polyethylene glycol: new insights into the reduction mechanism. *Journal of Nanoparticle Research,* 19**,** 113.

FOUNOU, R. C., FOUNOU, L. L. & ESSACK, S. Y. 2017. Clinical and economic impact of antibiotic resistance in developing countries: A systematic review and meta-analysis. *PloS one,* 12**,** e0189621.

FU, N., JI, M., ROUARD, M., YAN, H.-F. & GE, X.-J. 2022. Comparative plastome analysis of Musaceae and new insights into phylogenetic relationships. *BMC genomics,* 23**,** 223.

GONG, Y., JI, Y., LIU, F., LI, J. & CAO, Y. 2017. Cytotoxicity, oxidative stress and inflammation induced by ZnO nanoparticles in endothelial cells: interaction with palmitate or lipopolysaccharide. *Journal of Applied Toxicology,* 37**,** 895-901.

GUO, L., CHEN, H., HE, N. & DENG, Y. 2018. Effects of surface modifications on the physicochemical properties of iron oxide nanoparticles and their performance as anticancer drug carriers. *Chinese Chemical Letters,* 29**,** 1829-1833.

HANINI, A., SCHMITT, A., KACEM, K., CHAU, F., AMMAR, S. & GAVARD, J. 2011. Evaluation of iron oxide nanoparticle biocompatibility. *International journal of nanomedicine***,** 787-794.

HAO, X., XU, B., CHEN, H., WANG, X., ZHANG, J., GUO, R., SHI, X. & CAO, X. 2019. Stem cell-mediated delivery of nanogels loaded with ultrasmall iron oxide nanoparticles for enhanced tumor MR imaging. *Nanoscale,* 11**,** 4904-4910.

HERIZCHI, R., ABBASI, E., MILANI, M. & AKBARZADEH, A. 2016. Current methods for synthesis of gold nanoparticles. *Artificial Cells, Nanomedicine and Biotechnology,* 44**,** 596-602.

HOCHVALDOVÁ, L., VEČEŘOVÁ, R., KOLÁŘ, M., PRUCEK, R., KVÍTEK, L., LAPČÍK, L. & PANÁČEK, A. 2022. Antibacterial nanomaterials: Upcoming hope to overcome antibiotic resistance crisis. *Nanotechnology Reviews,* 11**,** 1115-1142.

HONG, G.-B. & JIANG, C.-J. 2017. Synthesis of SnO2 nanoparticles using extracts from Litsea cubeba fruits. *Materials Letters,* 194**,** 164-167.

HOOPER, D. C. & JACOBY, G. A. 2015. Mechanisms of drug resistance: quinolone resistance. *Annals of the New York academy of sciences,* 1354**,** 12-31.

HUANG, W.-Q., LIU, S.-R., HUANG, Z.-M., DONG, T.-G., WANG, G. & QIN, C.-J. 2015. Magic electron affection in preparation process of silicon nanocrystal. *Scientific Reports,* 5**,** 1-6.

HUDZICKI, J. 2009. Kirby-Bauer disk diffusion susceptibility test protocol. *American society for microbiology,* 15**,** 55-63.

HUH, A. J. & KWON, Y. J. 2011. "Nanoantibiotics": a new paradigm for treating infectious diseases using nanomaterials in the antibiotics resistant era. *Journal of controlled release,* 156**,** 128-145.

IBRAHIM, K., SAEED, A., KHALIL, S. & ALAM, A. 2023. ESTIMATION OF MINIMUM INHIBITORY CONCENTRATION OF ANTIBIOTICS USING MICRO-TITER PLATE METHOD FOR NATIVE MULTI DRUG RESISTANT GRAM NEGATIVE BACTERIA. *Pakistan Journal of Biotechnology,* 20**,** 1-9.

IBRAHIM, U., KAMARRUDIN, N., SUZIHAQUE, M. & ABD HASHIB, S. Local fruit wastes as a potential source of natural antioxidant: an overview. IOP conference series: materials science and engineering, 2017. IOP Publishing, 012040.

IV, M., TELISCHAK, N., FENG, D., HOLDSWORTH, S. J., YEOM, K. W. & DALDRUP-LINK, H. E. 2015. Clinical applications of iron oxide nanoparticles for magnetic resonance imaging of brain tumors. *Nanomedicine,* 10**,** 993-1008.

JACOB, P. J., MASARUDIN, M. J., HUSSEIN, M. Z. & RAHIM, R. A. 2019. Optimization of process parameters influencing the sustainable construction of iron oxide nanoparticles by a novel tropical wetlands Streptomyces spp. *Journal of Cleaner Production,* 232**,** 193-202.

JUSTUS, J. S., ROY, S. D. D., RAJ, A. M. E. & BOUOUDINA, M. 2019. The role of pH and effect of calcination temperature on polymorphs and properties of iron oxide nanoparticles. *International Journal of Nanoparticles,* 11**,** 62-78.

KANAGASUBBULAKSHMI, S. & KADIRVELU, K. 2017. Green synthesis of iron oxide nanoparticles using Lagenaria siceraria and evaluation of its antimicrobial activity. *Defence Life Science Journal,* 2**,** 422-427.

KARADE, V., DONGALE, T., SAHOO, S. C., KOLLU, P., CHOUGALE, A., PATIL, P. & PATIL, P. 2018. Effect of reaction time on structural and magnetic properties of green-synthesized magnetic nanoparticles. *Journal of Physics and Chemistry of Solids,* 120**,** 161-166.

KARPAGAVINAYAGAM, P. & VEDHI, C. 2019. Green synthesis of iron oxide nanoparticles using Avicennia marina flower extract. *Vacuum,* 160**,** 286-292.

KHALIL, A. T., OVAIS, M., ULLAH, I., ALI, M., KHAN SHINWARI, Z. & MAAZA, M. 2017. Biosynthesis of iron oxide (Fe2O3) nanoparticles via aqueous extracts of Sageretia thea (Osbeck.) and their pharmacognostic properties. *Green Chemistry Letters and Reviews,* 10**,** 186-201.

KHEZERLOU, A., ALIZADEH-SANI, M., AZIZI-LALABADI, M. & EHSANI, A. 2018. Nanoparticles and their antimicrobial properties against pathogens including bacteria, fungi, parasites and viruses. *Microbial pathogenesis,* 123**,** 505-526.

KIM, B., SEO, M.-R., KIM, J., KIM, Y., WIE, S.-H., KI, M., CHO, Y. K., LIM, S., LEE, J. S. & KWON, K. T. 2020. Molecular epidemiology of ciprofloxacin-resistant Escherichia coli isolated from community-acquired urinary tract infections in Korea. *Infection & chemotherapy,* 52**,** 194.

KOHANSKI, M. A., DEPRISTO, M. A. & COLLINS, J. J. 2010. Sublethal antibiotic treatment leads to multidrug resistance via radical-induced mutagenesis. *Molecular cell,* 37**,** 311-320.

KOOTI, M., SEDEH, A. N., MOTAMEDI, H. & REZATOFIGHI, S. E. 2018. Magnetic graphene oxide inlaid with silver nanoparticles as antibacterial and drug delivery composite. *Applied microbiology and biotechnology,* 102**,** 3607-3621.

KRIEDEMANN, B. & FESTER, V. 2015. Critical process parameters and their interactions on the continuous hydrothermal synthesis of ironoxide nanoparticles. *Chemical Engineering Journal,* 281**,** 312-321.

KRONSTAD, J. W. & CAZA, M. 2013. Shared and distinct mechanisms of iron acquisition by bacterial and fungal pathogens of humans. *Frontiers in Cellular and Infection Microbiology,* 4**,** 1-23.

KUCHIBHATLA, S. V., KARAKOTI, A. S., BAER, D. R., SAMUDRALA, S., ENGELHARD, M. H., AMONETTE, J. E., THEVUTHASAN, S. & SEAL, S. 2012. Influence of aging and environment on nanoparticle chemistry: implication to confinement effects in nanoceria. *The Journal of Physical Chemistry C,* 116**,** 14108-14114.

KULKARNI, S., MOHANTY, N., KADAM, N. N., SWAIN, N. & THAKUR, M. 2020. Green Synthesis to Develop Iron-Nano Formulations and Its Toxicity Assays. *Journal of Pharmacopuncture,* 23**,** 165-172.

KUMAR, E. R., JAYAPRAKASH, R., ARUNKUMAR, T. & KUMAR, S. 2013. Effect of reaction time on particle size and dielectric properties of manganese substituted CoFe2O4 nanoparticles. *Journal of Physics and Chemistry of Solids,* 74**,** 110-114.

KUMAR, M. K., KAUR, G. & KAUR, H. 2011. Phytochemical screening and Extraction. *INTERNATIONALE PHARMACEUTICA SCIENCIA,* 1**,** 98-106.

KUMAR, R., KUMAR, M. & LUTHRA, G. 2023. Fundamental approaches and applications of nanotechnology: A mini review. *Materials Today: Proceedings*.

KUSH, P., KUMAR, P., SINGH, R. & KAUSHIK, A. 2021. Aspects of high-performance and bio-acceptable magnetic nanoparticles for biomedical application. *Asian Journal of Pharmaceutical Sciences,* 16**,** 704-737.

KUYU, C. G. & TOLA, Y. B. 2018. Assessment of banana fruit handling practices and associated fungal pathogens in Jimma town market, southwest Ethiopia. *Food Science and Nutrition,* 6**,** 609-616.

LI, Q., HU, W., LI, L. & LI, Y. 2023. Interactions between organic matter and Fe oxides at soil micro-interfaces: Quantification, associations, and influencing factors. *Science of The Total Environment,* 855**,** 158710.

LI, Y., YANG, D., WANG, S., LI, C., XUE, B., YANG, L., SHEN, Z., JIN, M., WANG, J. & QIU, Z. 2018. The detailed bactericidal process of ferric oxide nanoparticles on E. coli. *Molecules,* 23**,** 606.

LIN, J., LI, Y., LI, Y., WU, H., YU, F., ZHOU, S., XIE, L., LUO, F., LIN, C. & HOU, Z. 2015. Drug/dye-loaded, multifunctional PEG–chitosan–iron oxide nanocomposites for methotraxate synergistically self-targeted cancer therapy and dual model imaging. *ACS applied materials & interfaces,* 7**,** 11908-11920.

LINSINGER, T., ROEBBEN, G., GILLILAND, D., CALZOLAI, L., ROSSI, F., GIBSON, P. & KLEIN, C. 2012. Requirements on measurements for the implementation of the European Commission definition of the term'nanomaterial'.

LIU, H., ZHANG, H., WANG, J. & WEI, J. 2020a. Effect of temperature on the size of biosynthesized silver nanoparticle: deep insight into microscopic kinetics analysis. *Arabian Journal of Chemistry,* 13**,** 1011-1019.

LIU, Y., YANG, G., JIN, S., XU, L. & ZHAO, C. X. 2020b. Development of high-drug-loading nanoparticles. *ChemPlusChem,* 85**,** 2143-2157.

LIVERMORE, D. M. 2011. Discovery research: The scientific challenge of finding new antibiotics. *Journal of Antimicrobial Chemotherapy,* 66**,** 1941-1944.

MADUBUONU, N., AISIDA, S. O., ALI, A., AHMAD, I., ZHAO, T.-K., BOTHA, S., MAAZA, M. & EZEMA, F. I. 2019. Biosynthesis of iron oxide nanoparticles via a composite of Psidium guavaja-Moringa oleifera and their antibacterial and photocatalytic study. *Journal of Photochemistry and Photobiology B: Biology,* 199**,** 111601.

MAHDAVI, M., AHMAD, M. B., HARON, M. J., NAMVAR, F., NADI, B., AB RAHMAN, M. Z. & AMIN, J. 2013. Synthesis, surface modification and characterisation of biocompatible magnetic iron oxide nanoparticles for biomedical applications. *Molecules,* 18**,** 7533-7548.

MAITY, D., SAHOO, S. R. & SAHA, S. 2023. Synthesis and Characterization of Nanomaterials for Electrochemical Sensors. *Recent Developments in Green Electrochemical Sensors: Design, Performance, and Applications.* ACS Publications.

MAJI, S. K., MUKHERJEE, N., MONDAL, A. & ADHIKARY, B. 2012. Synthesis, characterization and photocatalytic activity of α-Fe2O3 nanoparticles. *Polyhedron,* 33**,** 145-149.

MALEKI DIZAJ, S., LOTFIPOUR, F., BARZEGAR-JALALI, M., ZARRINTAN, M. H. & ADIBKIA, K. 2017. Ciprofloxacin HCl-loaded calcium carbonate nanoparticles: preparation, solid state characterization, and evaluation of antimicrobial effect against Staphylococcus aureus. *Artificial Cells, Nanomedicine and Biotechnology,* 45**,** 535-543.

MALHOTRA, N., LEE, J. S., LIMAN, R. A. D., RUALLO, J. M. S., VILLAFLORE, O. B., GER, T. R. & HSIAO, C. D. 2020. Potential toxicity of iron oxide magnetic nanoparticles: A review. *Molecules,* 25**,** 1-26.

MALIK, S., MUHAMMAD, K. & WAHEED, Y. 2023. Nanotechnology: A revolution in modern industry. *Molecules,* 28**,** 661.

MANATUNGA, D. C., DE SILVA, R. M., DE SILVA, K. N., DE SILVA, N., BHANDARI, S., YAP, Y. K. & COSTHA, N. P. 2017. pH responsive controlled release of anti-cancer hydrophobic drugs from sodium alginate and hydroxyapatite bi-coated iron oxide nanoparticles. *European Journal of Pharmaceutics and Biopharmaceutics,* 117**,** 29-38.

MANJUSHA, V., RAJEEV, M. & ANIRUDHAN, T. 2023. Magnetic nanoparticle embedded chitosan-based polymeric network for the hydrophobic drug delivery of paclitaxel. *International Journal of Biological Macromolecules,* 235**,** 123900.

MASADEH, M. M., ALZOUBI, K. H., KHABOUR, O. F. & AL-AZZAM, S. I. 2015. Ciprofloxacin-Induced Antibacterial Activity Is Attenuated by Phosphodiesterase Inhibitors. *Current Therapeutic Research - Clinical and Experimental,* 77**,** 14-17.

MEDINA, M. & CASTILLO-PINO, E. 2019. An introduction to the epidemiology and burden of urinary tract infections. *Therapeutic advances in urology,* 11**,** 1756287219832172.

MENICHETTI, A., MAVRIDI-PRINTEZI, A., MORDINI, D. & MONTALTI, M. 2023. Effect of Size, Shape and Surface Functionalization on the Antibacterial Activity of Silver Nanoparticles. *Journal of Functional Biomaterials,* 14**,** 244.

MISHRA, A., PRADHAN, D., HALDER, J., BISWASROY, P., RAI, V. K., DUBEY, D., KAR, B., GHOSH, G. & RATH, G. 2022. Metal nanoparticles against multi-drug-resistance bacteria. *Journal of Inorganic Biochemistry***,** 111938.

MOHSEN, E., EL-BORADY, O. M., MOHAMED, M. B. & FAHIM, I. S. 2020. Synthesis and characterization of ciprofloxacin loaded silver nanoparticles and investigation of their antibacterial effect. *Journal of Radiation Research and Applied Sciences,* 13**,** 416-425.

MORALES-DÍAZ, A. B., JUÁREZ-MALDONADO, A., MORELOS-MORENO, Á., GONZÁLEZ-MORALES, S. & BENAVIDES-MENDOZA, A. 2016. Biofabricación de nanopartículas de metales usando células vegetales o extractos de plantas. *Revista mexicana de ciencias agrícolas,* 7**,** 1211-1224.

MUBEEN, B., ANSAR, A. N., RASOOL, R., ULLAH, I., IMAM, S. S., ALSHEHRI, S., GHONEIM, M. M., ALZAREA, S. I., NADEEM, M. S. & KAZMI, I. 2021. Nanotechnology as a novel approach in combating microbes providing an alternative to antibiotics. *Antibiotics,* 10**,** 1473.

MÜHLBERGER, M., JANKO, C., UNTERWEGER, H., SCHREIBER, E., BAND, J., LEHMANN, C., DUDZIAK, D., LEE, G., ALEXIOU, C. & TIETZE, R. 2019. Functionalization of T lymphocytes for magnetically controlled immune therapy: Selection of suitable superparamagnetic iron oxide nanoparticles. *Journal of Magnetism and Magnetic Materials,* 473**,** 61-67.

NASRABADI, M., HALIMI, M. & NADAF, M. 2013. Phytochemical screeningand chemical composition of extract of Muscari neglectum. *Middle-East J Sci Res,* 14**,** 566-9.

NATRAYAN, L., RAO, Y. S., VAIDYA, G., BHATTACHARYA, S., KALIAPPAN, S., PATIL, P. P. & PARAMASIVAM, P. 2023. Biosynthesis of Iron Oxide Nanoparticles Using Leaf Extract of Ruellia tuberosa: Mechanical and Dynamic Mechanical Behaviour Kevlar-Based Hybrid Epoxy Composites. *Bioinorganic Chemistry and Applications,* 2023.

NAVYA, P., KAPHLE, A., SRINIVAS, S., BHARGAVA, S. K., ROTELLO, V. M. & DAIMA, H. K. 2019. Current trends and challenges in cancer management and therapy using designer nanomaterials. *Nano convergence,* 6**,** 1-30.

NAWAZ, A., ALI, S. M., RANA, N. F., TANWEER, T., BATOOL, A., WEBSTER, T. J., MENAA, F., RIAZ, S., REHMAN, Z. & BATOOL, F. 2021a. Ciprofloxacin-loaded gold

nanoparticles against antimicrobial resistance: an in vivo assessment. *Nanomaterials*, 11**,** 3152.

NAWAZ, A., ALI, S. M., RANA, N. F., TANWEER, T., BATOOL, A., WEBSTER, T. J., MENAA, F., RIAZ, S., REHMAN, Z., BATOOL, F., FATIMA, M., MARYAM, T., SHAFIQUE, I., SALEEM, A. & IQBAL, A. 2021b. Ciprofloxacin-loaded gold nanoparticles against antimicrobial resistance: An in vivo assessment. *Nanomaterials,* 11.

NAZ, S., ISLAM, M., TABASSUM, S., FERNANDES, N. F., BLANCO, E. J. C. D. & ZIA, M. 2019a. Green Synthesis of Hematite (α-Fe2O3) Nanoparticles using Rhus punjabensis extract and their biomedical prospect in pathogenic diseases and cancer. *Journal of Molecular Structure*.

NAZ, S., ISLAM, M., TABASSUM, S., FERNANDES, N. F., DE BLANCO, E. J. C. & ZIA, M. 2019b. Green synthesis of hematite (α-Fe2O3) nanoparticles using Rhus punjabensis extract and their biomedical prospect in pathogenic diseases and cancer. *Journal of Molecular Structure,* 1185**,** 1-7.

NAZ, S. S., ISLAM, N. U., SHAH, M. R., ALAM, S. S., IQBAL, Z., BERTINO, M., FRANZEL, L. & AHMED, A. 2013. Enhanced biocidal activity of Au nanoparticles synthesized in one pot using 2, 4-dihydroxybenzene carbodithioic acid as a reducing and stabilizing agent. *Journal of nanobiotechnology,* 11**,** 1-9.

NEYESTANI, Z., KHADEMI, F., TEIMOURPOUR, R., AMANI, M. & ARZANLOU, M. 2023. Prevalence and mechanisms of ciprofloxacin resistance in Escherichia coli isolated from hospitalized patients, healthy carriers, and wastewaters in Iran. *BMC microbiology*, 23**,** 191.

NICULESCU, A.-G., CHIRCOV, C. & GRUMEZESCU, A. M. 2022. Magnetite nanoparticles: Synthesis methods–A comparative review. *Methods,* 199**,** 16-27.

NISAR, M., KHAN, S. A., QAYUM, M., KHAN, A., FAROOQ, U., JAAFAR, H. Z., ZIA-UL-HAQ, M. & ALI, R. 2016. Robust synthesis of ciprofloxacin-capped metallic nanoparticles and their urease inhibitory assay. *Molecules,* 21**,** 411.

NWAMEZIE, O. 2018. Green synthesis of iron nanoparticles using flower extract of Piliostigma thonningii and their antibacterial activity evaluation. *Chemistry International,* 4**,** 60-66.

PADAM, B. S., TIN, H. S., CHYE, F. Y. & ABDULLAH, M. I. 2014. Banana by-products: an under-utilized renewable food biomass with great potential. *Journal of Food Science and Technology,* 51**,** 3527-3545.

PATRASCU, J. M., NEDELCU, I. A., SONMEZ, M., FICAI, D., FICAI, A., VASILE, B. S., UNGUREANU, C., ALBU, M. G., ANDOR, B., ANDRONESCU, E. & RUSU, L. C. 2015. Composite Scaffolds Based on Silver Nanoparticles for Biomedical Applications. *Journal of Nanomaterials,* 2015.

PELGRIFT, R. Y. & FRIEDMAN, A. J. 2013. Nanotechnology as a therapeutic tool to combat microbial resistance. *Advanced drug delivery reviews,* 65**,** 1803-1815.

PINTO, R. M., LOPES-DE-CAMPOS, D., MARTINS, M. C. L., VAN DIJCK, P., NUNES, C. & REIS, S. 2019. Impact of nanosystems in Staphylococcus aureus biofilms treatment. *FEMS Microbiology Reviews,* 43**,** 622-641.

PRUSTY, K. & SWAIN, S. K. 2019. Release of ciprofloxacin drugs by nano gold embedded cellulose grafted polyacrylamide hybrid nanocomposite hydrogels. *International journal of biological macromolecules,* 126**,** 765-775.

PUGAZHENDHI, A., KUMAR, S. S., MANIKANDAN, M. & SARAVANAN, M. 2018. Photocatalytic properties and antimicrobial efficacy of Fe doped CuO nanoparticles against the pathogenic bacteria and fungi. *Microbial Pathogenesis,* 122**,** 84-89.

PUSHCHAROVSKY, D. Y. 2019. Iron and Its Compounds in the Earth's Core: New Data and Ideas. *Geochemistry International,* 57**,** 941-955.

RAFI, M. M., AHMED, K. S. Z., NAZEER, K. P., SIVA KUMAR, D. & THAMILSELVAN, M. 2015. Synthesis, characterization and magnetic properties of hematite (α-Fe2O3) nanoparticles on polysaccharide templates and their antibacterial activity. *Applied Nanoscience (Switzerland),* 5**,** 515-520.

RAI, A., COMUNE, M. & FERREIRA, L. 2019. Nanoparticle-based drug delivery systems: Promising approaches against bacterial infections. *Antibacterial Drug Discovery to Combat MDR: Natural Compounds, Nanotechnology and Novel Synthetic Sources***,** 605-633.

RAJENDRAN, K. & SEN, S. 2016. Optimization of process parameters for the rapid biosynthesis of hematite nanoparticles. *J Photochem Photobiol B,* 159**,** 82-7.

RAMESH, R., YAMINI, V., RAJKUMAR, D., SUNDARAM, S. J., LAKSHMI, D. & KHAN, F. L. A. 2021. Biogenic synthesis of α-Fe2O3 nanoparticles using Plectranthus amboinicus leaf extract. *Materials Today: Proceedings,* 36**,** 453-458.

RATHER, M. Y. & SUNDARAPANDIAN, S. 2020. Magnetic iron oxide nanorod synthesis by Wedelia urticifolia (Blume) DC. leaf extract for methylene blue dye degradation. *Applied Nanoscience,* 10**,** 2219-2227.

REIS, A. C. C., SANTOS, S. R. D. S., SOUZA, S. C. D., SALDANHA, M. G., PITANGA, T. N. & OLIVEIRA, R. R. 2016. Ciprofloxacin resistance pattern among bacteria isolated from patients with community-acquired urinary tract infection. *Revista do Instituto de Medicina Tropical de São Paulo,* 58.

RITA, W. S., SWANTARA, I. M. D., ASTITI ASIH, I. A. R. & PUSPAWATI, N. M. 2020. ANTIBACTERIAL ACTIVITY AND ANTIOXIDANT CAPACITY OF SELECTED LOCAL BANANA PEEL (Musa sp.) METHANOL EXTRACTS CULTIVATED IN BALI. *International Journal of Agriculture, Environment and Bioresearch,* 05**,** 242-251.

ROGHINI, R. & VIJAYALAKSHMI, K. 2018. Phytochemical screening, quantitative analysis of flavonoids and minerals in ethanolic extract of Citrus paradisi. *International Journal of Pharmaceutical Sciences and Research,* 9**,** 4859-4864.

ROSE, I., SATHISH, R., RAJENDRAN, A. J. & SAGAYARAJ, P. 2016. Effect of reaction time on the synthesis of cadmium selenide nanoparticles and the efficiency of solar cell. *J. Mater. Environ. Sci,* 7**,** 1589-1596.

ROSS, D. L. & RILEY, C. M. 1990. Aqueous solubilities of some variously substituted quinolone antimicrobials. *International Journal of Pharmaceutics,* 63**,** 237-250.

ROSSIGNOL, L., VAUX, S., MAUGAT, S., BLAKE, A., BARLIER, R., HEYM, B., LE STRAT, Y., BLANCHON, T., HANSLIK, T. & COIGNARD, B. 2017. Incidence of urinary tract infections and antibiotic resistance in the outpatient setting: a cross-sectional study. *Infection,* 45**,** 33-40.

SAIF, S., TAHIR, A. & CHEN, Y. 2016. Green synthesis of iron nanoparticles and their environmental applications and implications. *Nanomaterials,* 6**,** 209.

SAMUEL, M. S., RAVIKUMAR, M., JOHN J, A., SELVARAJAN, E., PATEL, H., CHANDER, P. S., SOUNDARYA, J., VUPPALA, S., BALAJI, R. &

CHANDRASEKAR, N. 2022. A review on green synthesis of nanoparticles and their diverse biomedical and environmental applications. *Catalysts,* 12**,** 459.

SAQIB, S., MUNIS, M. F. H., ZAMAN, W., ULLAH, F., SHAH, S. N., AYAZ, A., FAROOQ, M. & BAHADUR, S. 2019. Synthesis, characterization and use of iron oxide nano particles for antibacterial activity. *Microscopy research and technique,* 82**,** 415-420.

SARDOS, J., PERRIER, X., DOLEŽEL, J., HŘIBOVÁ, E., CHRISTELOVÁ, P., VAN DEN HOUWE, I., KILIAN, A. & ROUX, N. 2016. DArT whole genome profiling provides insights on the evolution and taxonomy of edible Banana (Musa spp.). *Annals of Botany,* 118**,** 1269-1278.

SATAR, R., IIZHAR, S. A., RASOOL, M., PUSHPARAJ, P. N. & ANSARI, S. A. 2016. Investigating the antibacterial potential of agarose nanoparticles synthesized by nanoprecipitation technology. *Polish Journal of Chemical Technology,* 18**,** 9-12.

SELVANAYAKI, R., RAMESHBABU, M., MUTHUPANDI, S., RAZIA, M., FLORENCE, S. S., RAVICHANDRAN, K. & PRABHA, K. 2022. Structural, optical and electrical conductivity studies of pure and Fe doped ZincOxide (ZnO) nanoparticles. *Materials Today: Proceedings,* 49**,** 2628-2631.

SELVARAJ, R., PAI, S., VINAYAGAM, R., VARADAVENKATESAN, T., KUMAR, P. S., DUC, P. A. & RANGASAMY, G. 2022. A recent update on green synthesized iron and iron oxide nanoparticles for environmental applications. *Chemosphere***,** 136331.

SENAPATI, S., MAHANTA, A. K., KUMAR, S. & MAITI, P. 2018. Controlled drug delivery vehicles for cancer treatment and their performance. *Signal Transduction and Targeted Therapy,* 3**,** 1-19.

SHAIKH, J. R. & PATIL, M. 2020. Qualitative tests for preliminary phytochemical screening: An overview. *International Journal of Chemical Studies,* 8**,** 603-608.

SHARMA, D., LEDWANI, L., MEHROTRA, T., KUMAR, N., PERVAIZ, N. & KUMAR, R. 2020a. Biosynthesis of hematite nanoparticles using Rheum emodi and their antimicrobial and anticancerous effects in vitro. *J Photochem Photobiol B,* 206**,** 111841.

SHARMA, D., LEDWANI, L., MEHROTRA, T., KUMAR, N., PERVAIZ, N. & KUMAR, R. 2020b. Biosynthesis of hematite nanoparticles using Rheum emodi and their antimicrobial and anticancerous effects in vitro. *Journal of Photochemistry and Photobiology B: Biology,* 206**,** 111841.

SHEN, S., ZHOU, J., DONG, C. L., HU, Y., TSENG, E. N., GUO, P., GUO, L. & MAO, S. S. 2014. Surface engineered doping of hematite nanorod arrays for improved photoelectrochemical water splitting. *Scientific Reports,* 4**,** 1-9.

SHRESTHA, P., COOPER, B. S., COAST, J., OPPONG, R., DO THI THUY, N., PHODHA, T., CELHAY, O., GUERIN, P. J., WERTHEIM, H. & LUBELL, Y. 2018. Enumerating the economic cost of antimicrobial resistance per antibiotic consumed to inform the evaluation of interventions affecting their use. *Antimicrobial Resistance & Infection Control,* 7**,** 1-9.

SIAL, T. A., KHAN, M. N., LAN, Z., KUMBHAR, F., YING, Z., ZHANG, J., SUN, D. & LI, X. 2019. Contrasting effects of banana peels waste and its biochar on greenhouse gas emissions and soil biochemical properties. *Process Safety and Environmental Protection,* 122**,** 366-377.

SINGH, R., SMITHA, M. S. & SINGH, S. P. 2014. The role of nanotechnology in combating multi-drug resistant bacteria. *Journal of Nanoscience and Nanotechnology,* 14**,** 4745-4756.

SIRIVISOOT, S. & HARRISON, B. S. 2015. Magnetically stimulated ciprofloxacin release from polymeric microspheres entrapping iron oxide nanoparticles. *International journal of nanomedicine,* 10**,** 4447.

SOLIMAN, N. M., SHAKEEL, F., HAQ, N., ALANAZI, F. K., ALSHEHRI, S., BAYOMI, M., ALENAZI, A. S. & ALSARRA, I. A. 2022. Development and optimization of ciprofloxacin HCl-loaded chitosan nanoparticles using box–behnken experimental design. *Molecules,* 27**,** 4468.

SONAM, M., SINGH, R. P. & POOJA, S. 2017. Phytochemical screening and TLC profiling of various extracts of Reinwardtia indica. *International Journal of Pharmacognosy and Phytochemical Research,* 9**,** 523-527.

SONI, N. & PRAKASH, S. 2011. Factors affecting the geometry of silver nanoparticles synthesis in Chrysosporium tropicum and Fusarium oxysporum. *Am J Nanotechnol,* 2**,** 112-121.

SREEDHARAN, S. M. & SINGH, R. 2019. Ciprofloxacin functionalized biogenic gold nanoflowers as nanoantibiotics against pathogenic bacterial strains. *International journal of nanomedicine***,** 9905-9916.

SREEKANTH, T., NAGAJYOTHI, P., MUTHURAMAN, P., ENKHTAIVAN, G., VATTIKUTI, S., TETTEY, C., KIM, D. H., SHIM, J. & YOO, K. 2018. Ultra-sonication-assisted silver nanoparticles using Panax ginseng root extract and their anti-cancer and antiviral activities. *Journal of Photochemistry and Photobiology B: Biology,* 188**,** 6-11.

STANICKI, D., VANGIJZEGEM, T., TERNAD, I. & LAURENT, S. 2022. An update on the applications and characteristics of magnetic iron oxide nanoparticles for drug delivery. *Expert Opinion on Drug Delivery,* 19**,** 321-335.

SULTANA, M. & TOAHA, M. 2021. Study of uropathogens in patients with urinary tract infection and their antibiotic sensitivity profile. *Australian Journal of Science and Technology,* 5**,** 403-409.

SUMATHY, V., LACHUMY, S. J., ZAKARIA, Z. & SASIDHARAN, S. 2011. In vitro bioactivity and phytochemical screening of Musa acuminata flower. *Pharmacologyonline,* 2**,** 118-127.

SUMEDHA, S. & ANDREA, J.-L. Y. 2016. Subnanometric Roughness Affects the Deposition and Mobile Adhesion of Escherichia coli on Silanized Glass Surfaces. *Langmuir* 32**,** 5422-5433.

SUNDARA SELVAM, P. S., GOVINDAN, S., PERUMAL, B. & KANDAN, V. 2020. Screening of In Vitro Antibacterial Property of Hematite (α-Fe2O3) Nanoparticles: A Green Approach. *Iranian Journal of Science and Technology, Transactions A: Science,* 45**,** 177-187.

SUSANAH, R. W., RETNO, K. & MADE DIRA, S. I. 2018. Total phenolic and flavonoid contents and antimicrobial activity of acorus calamus L. Rhizome ethanol extract. *Research Journal of Chemistry and Environment,* 22**,** 65-70.

TEOW, S. Y., WONG, M. M. T., YAP, H. Y., PEH, S. C. & SHAMELI, K. 2018. Bactericidal properties of plants-derived metal and metal oxide nanoparticles (NPs). *Molecules,* 23**,** 1-23.

TERRENI, M., TACCANI, M. & PREGNOLATO, M. 2021. New antibiotics for multidrug-resistant bacterial strains: latest research developments and future perspectives. *Molecules,* 26**,** 2671.

TOM, R. T., SURYANARAYANAN, V., REDDY, P. G., BASKARAN, S. & PRADEEP, T. 2004. Ciprofloxacin-Protected Gold Nanoparticles. *Langmuir,* 20**,** 1909-1914.

TONG, D. Q., GILL, T. E., SPRIGG, W. A., VAN PELT, R. S., BAKLANOV, A. A., BARKER, B. M., BELL, J. E., CASTILLO, J., GASSÓ, S. & GASTON, C. J. 2023. Health and safety effects of airborne soil dust in the Americas and beyond. *Reviews of Geophysics,* 61**,** e2021RG000763.

TOPAL, G. R., DEVRIM, B., ERYILMAZ, M. & BOZKIR, A. 2018. Design of ciprofloxacin-loaded nano-and microcomposite particles for dry powder inhaler formulations: preparation, in vitro characterisation, and antimicrobial efficacy. *Journal of Microencapsulation,* 35**,** 533-547.

TYAGI, P. K., GUPTA, S., TYAGI, S., KUMAR, M., PANDISELVAM, R., DAŞTAN, S. D., SHARIFI-RAD, J., GOLA, D. & ARYA, A. 2021. Green synthesis of iron nanoparticles from spinach leaf and banana peel aqueous extracts and evaluation of antibacterial potential. *Journal of Nanomaterials,* 2021**,** 1-11.

US DEPARTMENT OF HEALTH AND HUMAN SERVICES 2019. *Antibiotic resistance threats in the United States, 2019,* US Department of Health and Human Services, Centres for Disease Control and ….

VASSALLO, A., SILLETTI, M. F., FARAONE, I. & MILELLA, L. 2020. Nanoparticulate Antibiotic Systems as Antibacterial Agents and Antibiotic Delivery Platforms to Fight Infections. *Journal of Nanomaterials,* 2020.

VIHODCEVA, S., ŠUTKA, A., SIHTMÄE, M., ROSENBERG, M., OTSUS, M., KURVET, I., SMITS, K., BIKSE, L., KAHRU, A. & KASEMETS, K. 2021. Antibacterial activity of positively and negatively charged hematite (α-fe2 o3) nanoparticles to escherichia coli, staphylococcus aureus and vibrio fischeri. *Nanomaterials,* 11**,** 1-26.

VINAYAGAM, R., PAI, S., VARADAVENKATESAN, T., NARASIMHAN, M. K., NARAYANASAMY, S. & SELVARAJ, R. 2020. Structural characterization of green synthesized α-Fe2O3 nanoparticles using the leaf extract of Spondias dulcis. *Surfaces and Interfaces,* 20**,** 100618.

VOL, S., APRIL, N., ALAWKALLY, N. M., EL, S., FAKRON, A., IBRAHIM, H. K. & SULIMAN, N. A. 2022. Risk Factors for Ciprofloxacin and Gentamycin Resistance among Gram Positive and Gram Negative Bacteria Isolated from Community-Acquired

Urinary Tract Infections in Benghazi City. *Scientific Journal for the Faculty of Science - Sirte University,* 2**,** 76-87.

WANG, C. 2023. Reconstituted Lipid Nanoparticles from Cells/Tissues for Drug Delivery in Cancer. *Molecular Pharmaceutics,* 20**,** 2891-2898.

WANG, Y., WANG, Y., SU, L., LUAN, Y., DU, X. & ZHANG, X. 2019. Effect of surface topology morphologies of silica nanocarriers on the loading of Ag nanoparticles and antibacterial performance. *Journal of Alloys and Compounds,* 783**,** 136-144.

WANG, Z., FANG, C. & MALLAVARAPU, M. 2015. Characterization of iron–polyphenol complex nanoparticles synthesized by Sage (Salvia officinalis) leaves. *Environmental Technology & Innovation,* 4**,** 92-97.

WU, Z., CHAN, B., LOW, J., CHU, J. J. H., HEY, H. W. D. & ANDY, T. 2022. Microbial resistance to nanotechnologies: An important but understudied consideration using antimicrobial nanotechnologies in orthopaedic implants, Bioactive Materials. *Bioactive materials,* 16**,** 249-270.

XIE, W., GUO, Z., GAO, F., GAO, Q., WANG, D., LIAW, B.-S., CAI, Q., SUN, X., WANG, X. & ZHAO, L. 2018. Shape-, size-and structure-controlled synthesis and biocompatibility of iron oxide nanoparticles for magnetic theranostics. *Theranostics,* 8**,** 3284.

YAN, H. & ZHANG, B. 2011. In vitro cytotoxicity of monodispersed hematite nanoparticles on Hek 293 cells. *Materials Letters,* 65**,** 815-817.

YI, Y., TU, G., TSANG, P. E., XIAO, S. & FANG, Z. 2019. Green synthesis of iron-based nanoparticles from extracts of Nephrolepis auriculata and applications for Cr (VI) removal. *Materials Letters,* 234**,** 388-391.

YIU, H. H., PICKARD, M. R., OLARIU, C. I., WILLIAMS, S. R., CHARI, D. M. & ROSSEINSKY, M. J. 2012. Fe 3 O 4-PEI-RITC magnetic nanoparticles with imaging and gene transfer capability: development of a tool for neural cell transplantation therapies. *Pharmaceutical research,* 29**,** 1328-1343.

YOONUS, J., RESMI, R. & BEENA, B. 2021. Evaluation of antibacterial and anticancer activity of green synthesized iron oxide (α-Fe2O3) nanoparticles. *Materials Today: Proceedings,* 46**,** 2969-2974.

YU, H., WANG, Y., WANG, S., LI, X., LI, W., DING, D., GONG, X., KEIDAR, M. & ZHANG, W. 2018. Paclitaxel-loaded core–shell magnetic nanoparticles and cold

atmospheric plasma inhibit non-small cell lung cancer growth. *ACS applied materials & interfaces,* 10**,** 43462-43471.

YU, Z., GAO, L., CHEN, K., ZHANG, W., ZHANG, Q., LI, Q. & HU, K. 2021. Nanoparticles: a new approach to upgrade cancer diagnosis and treatment. *Nanoscale Research Letters,* 16**,** 88.

ZAFAR, N., UZAIR, B., MENAA, F., KHAN, B. A., NIAZI, M. B. K., ALARYANI, F. S., MAJRASHI, K. A. & SAJJAD, S. 2022. Moringa concanensis-Mediated Synthesis and Characterizations of Ciprofloxacin Encapsulated into Ag/TiO2/Fe2O3/CS Nanocomposite: A Therapeutic Solution against Multidrug Resistant E. coli Strains of Livestock Infectious Diseases. *Pharmaceutics,* 14**,** 1719.

ZAFAR, N., UZAIR, B., NIAZI, M. B. K., MENAA, F., SAMIN, G., KHAN, B. A., IQBAL, H. & MENAA, B. 2021. Green Synthesis of Ciprofloxacin-Loaded Cerium Oxide/Chitosan Nanocarrier and its Activity Against MRSA-Induced Mastitis. *Journal of Pharmaceutical Sciences,* 110**,** 3471-3483.

ZAINI, H. M., ROSLAN, J., SAALLAH, S., MUNSU, E., SULAIMAN, N. S. & PINDI, W. 2022. Banana peels as a bioactive ingredient and its potential application in the food industry. *Journal of Functional Foods,* 92**,** 105054.

ZAKARIYA, N. A., JUSOF, W. H. W. & MAJEED, S. 2022. Green approach for iron oxide nanoparticles synthesis: application in antimicrobial and anticancer-an updated review. *Karbala International Journal of Modern Science,* 8**,** 421-437.

ZBORIL, R., MASHLAN, M. & PETRIDIS, D. 2002. Iron (III) Oxides from Thermal Processes s Synthesis. *Chemistry Materials,* 14**,** 969-982.

ZHOU, G. & LV, X. 2020. Ciprofloxacin resistance in hospital and community-acquired urinary tract infections by Escherichia coli: A systematic review and meta-analysis. *bioRxiv*.

9. Appendixes

Appendix I: Calibration curve of ciprofloxacin in distilled water

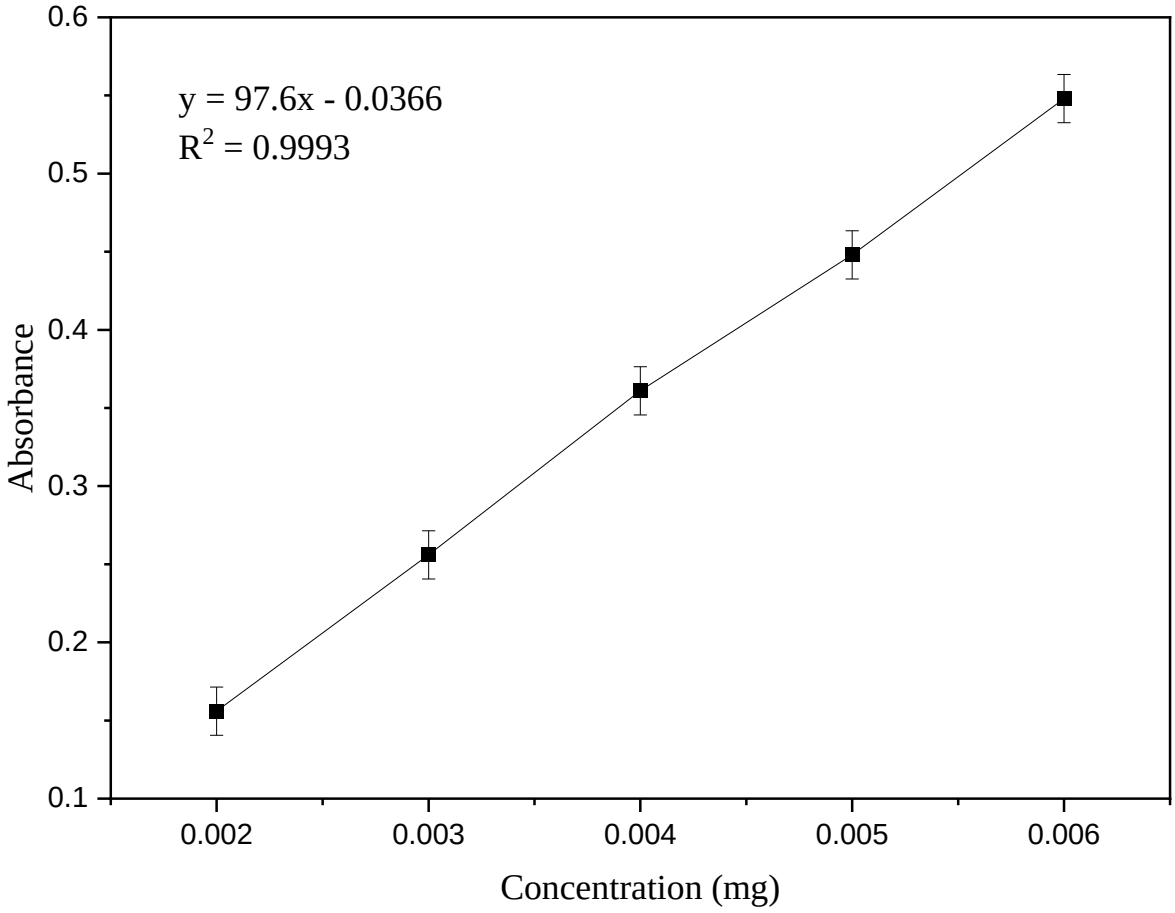

Appendix II: Calibration curve of ciprofloxacin in buffer solution of pH, (A) 1.2, (B) 6.8, and (C) 7.4.

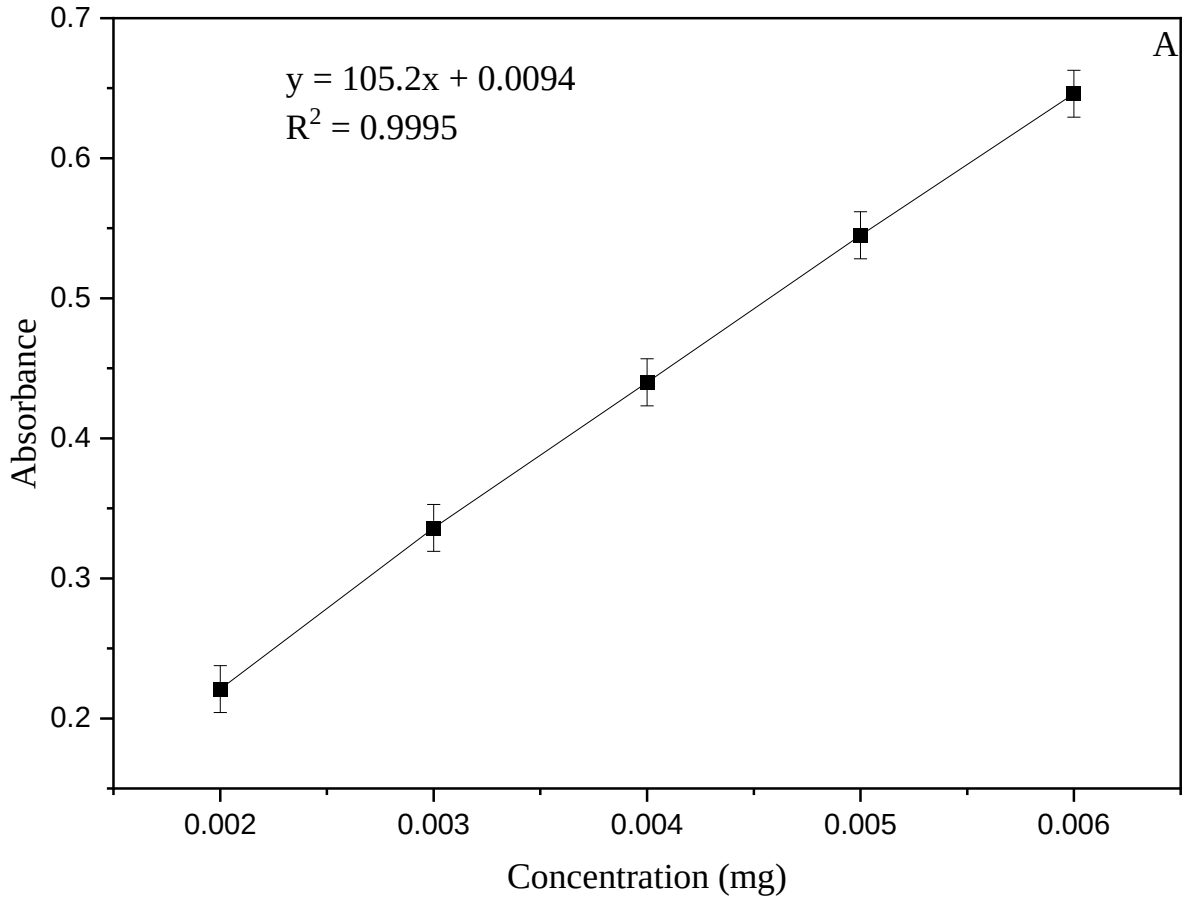

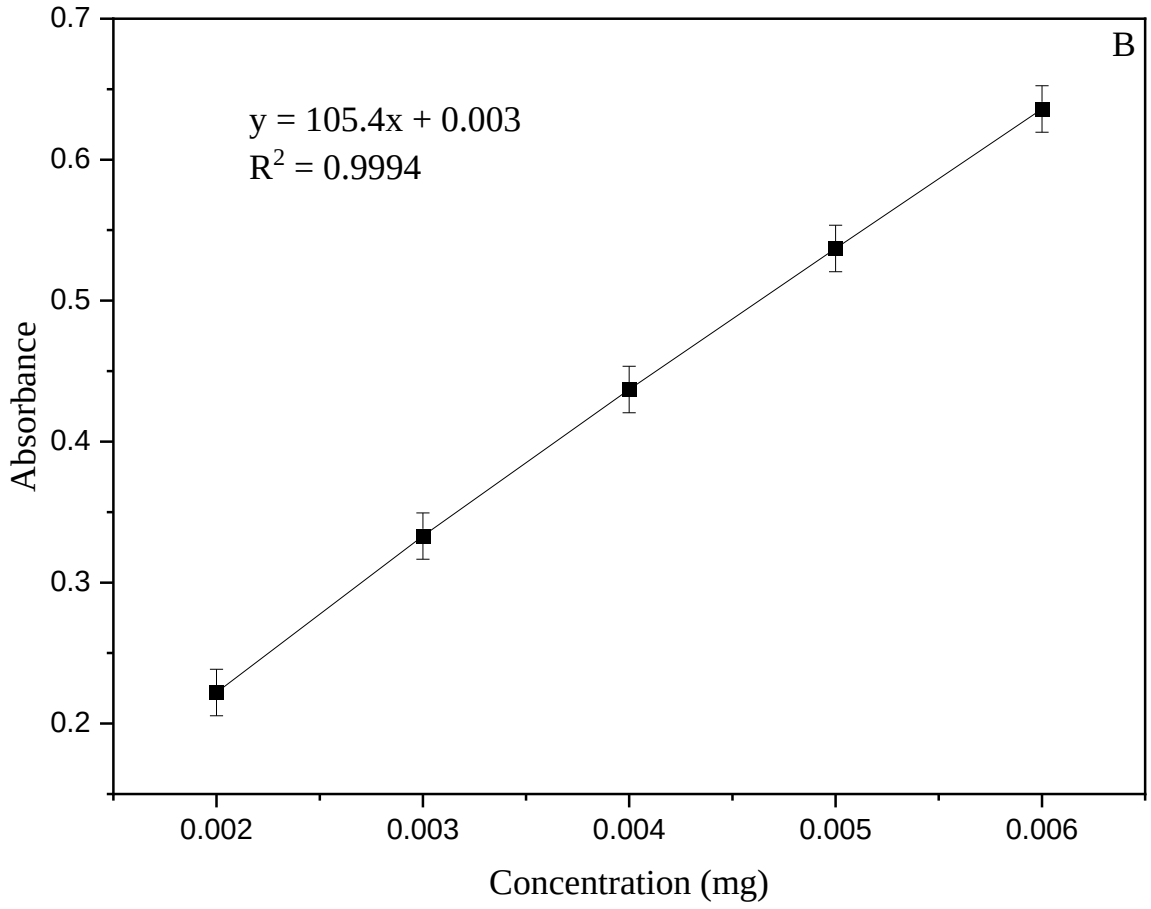
B
y = 105.4x + 0.003
R2 = 0.9994
Absorbance
0.7
0.6
0.5
0.4
0.3
0.2
0.002
0.003
0.004
0.005
0.006
Concentration (mg)

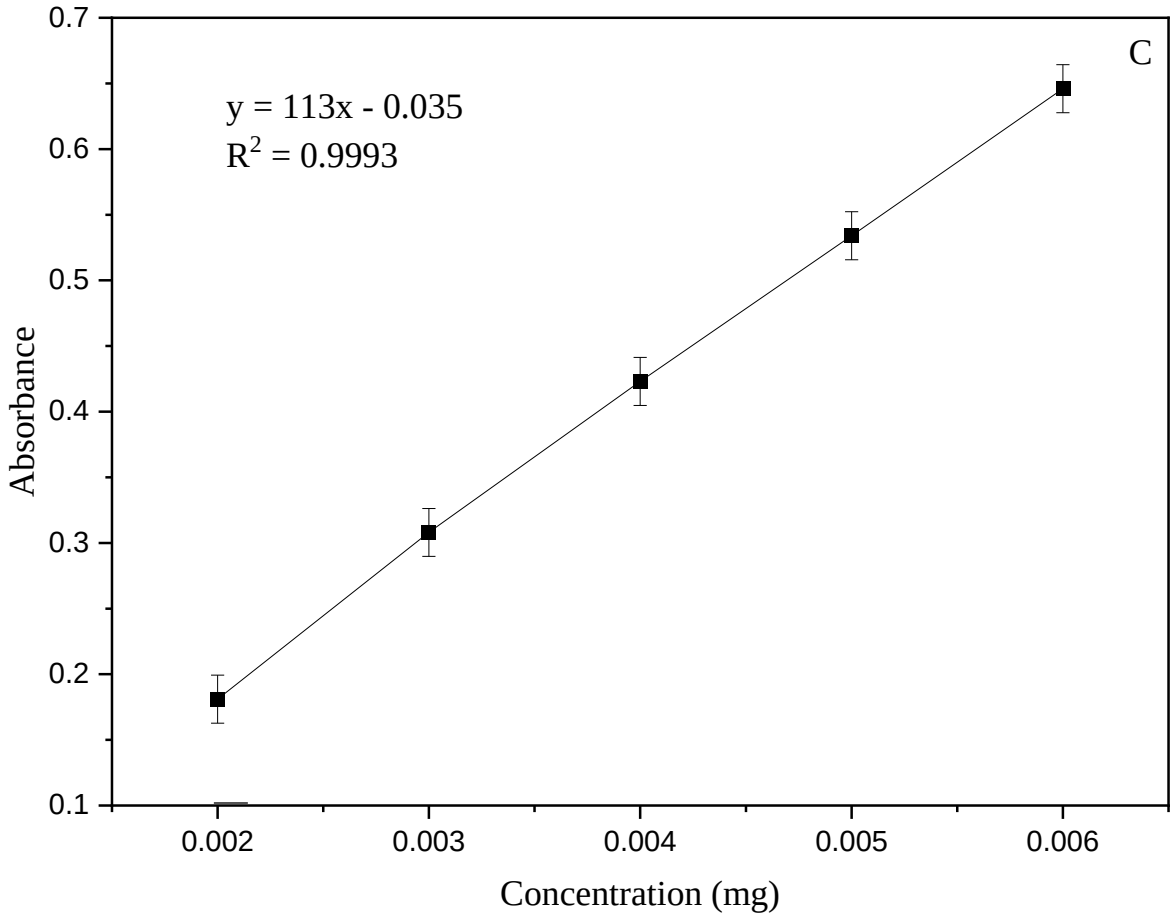
C
y = 113x - 0.035
R2 = 0.9993
Absorbance
Concentration (mg)
0.7
0.6
0.5
0.4
0.3
0.2
0.1
0.002
0.003
0.004
0.005
0.006